NEOPLASIA
www.neoplasia.com

Volume 13 Number 12 December 2011 pp. 1171–1182 **1171**

Ras-Related Tumorigenesis Is Suppressed by BNIP3-Mediated Autophagy through Inhibition of Cell Proliferation[1,2]

Shan-Ying Wu*, Sheng-Hui Lan*, Da-En Cheng†, Wei-Kai Chen†, Cheng-Huang Shen‡, Ying-Ray Lee‡, Roberto Zuchini§,¶ and Hsiao-Sheng Liu*,†,#

*Institute of Basic Medical Sciences, College of Medicine, National Cheng Kung University, Tainan, Taiwan; †Department of Microbiology and Immunology, College of Medicine, National Cheng Kung University, Tainan, Taiwan; ‡Department of Urology, Chia-Yi Christian Hospital, Chia-Yi, Taiwan; §Graduate Institute of Clinical Medicine, National Cheng Kung University, Tainan, Taiwan; ¶Department of Internal Medicine, National Cheng Kung University, Tainan, Taiwan; #Center of Infectious Disease and Signaling Research Center, National Cheng Kung University, Tainan, Taiwan

Abstract

Autophagy plays diverse roles in Ras-related tumorigenesis. H-*ras*^{val12} induces autophagy through multiple signaling pathways including Raf-1/ERK pathway, and various ERK downstream molecules of autophagy have been reported. In this study, Bcl-2/adenovirus E1B 19-kDa–interacting protein 3 (BNIP3) is identified as a downstream transducer of the Ras/Raf/ERK signaling pathway to induce autophagy. BNIP3 was upregulated by H-*ras*^{val12} at the transcriptional level to compete with Beclin 1 for binding with Bcl-2. H-*ras*^{val12}–induced autophagy suppresses cell proliferation demonstrated both *in vitro* and *in vivo* by expression of ectopic BNIP3, Atg5, or interference RNA of BNIP3 (siBNIP3) and Atg5 (shAtg5) using mouse NIH3T3 and embryo fibroblast cells. H-*ras*^{val12} induces different autophagic responses depending on the duration of Ras overexpression. After a short time (48 hours) of Ras overexpression, autophagy inhibits cell proliferation. In contrast, a longer time (2 weeks) of Ras overexpression, cell proliferation was enhanced by autophagy. Furthermore, overexpression of mutant Ras, BNIP3, and LC3-II was detected in bladder cancer T24 cells and the tumor parts of 75% of bladder cancer specimens indicating a positive correlation between autophagy and tumorigenesis. Taken together, our mouse model demonstrates a balance between BNIP3-mediated autophagy and H-*ras*^{val12}–induced tumor formation and reveals that H-*ras*^{val12} induces autophagy in a BNIP3-dependent manner, and the threshold of autophagy plays a decisive role in H-*ras*^{val12}–induced tumorigenesis. Our findings combined with others' reports suggest a new therapeutic strategy against Ras-related tumorigenesis by negative or positive regulation of autophagic activity, which is determined by the level of autophagy and tumor progression stages.

Neoplasia (2011) 13, 1171–1182

Address all correspondence to: Dr. Hsiao-Sheng Liu, Department of Microbiology and Immunology, College of Medicine, National Cheng Kung University, Tainan, Taiwan. E-mail: a713@mail.ncku.edu.tw

[1]This work was supported by grants from National Science Council NSC-96-2628-B-006-003-MY3 and NSC-99-2745-B-006-002. The authors declare that they have no competing interests.

[2]This article refers to supplementary materials, which are designated by Figures W1 to W13 and are available online at www.neoplasia.com.

Received 30 June 2011; Revised 7 November 2011; Accepted 12 November 2011

DOI 10.1593/neo.11888

Introduction

Autophagy is a cellular stress–adaptive process in which double-membrane structures called autophagosomes engulf cytosolic organelles and proteins, fuse with lysosomes, and degrade them to provide energy to the cell [1,2]. This whole process is known as autophagic flux [3]. The autophagosome contains the microtubule-associated protein light chain 3 (LC3), which is the human homolog of Atg8 in yeast. It is found as LC3-I in the cytosol, and as LC3-II (the lipidative derivate of LC3-I) on autophagosomal membranes. Within the autophagosome and lysosomal structures, there is also the polyubiquitin-binding protein p62/SQSTM1 (also named sequestosome 1 [SQSTM1]), which yields protein bodies that can also reside free in the cytosol and nucleus. During the autophagic flux, p62 recruits LC3 to form a complex that is transported to the autophagosomes and subsequently degraded in an organelle created by the fusion of autophagosomes and lysosomes called autophagolysosome [4]. Inhibiting this fusion leads to accumulation of the LC3 and p62 proteins [5].

Autophagy can be activated by various stimuli including hypoxia during tumor formation [6]. Furthermore, autophagy spatially and temporally regulates tumor development by suppressing tumor growth through regulating cell proliferation at the early stages of tumorigenesis [7]. At later stages, cancer cells in the central area of the tumor mass are poorly vascularized and undergo autophagy to overcome low-nutrient conditions [8]. However, the underlying mechanisms by which diverse types of stresses induce autophagy during cell transformation and tumorigenesis remain controversial and require further studies.

Ras proto-oncogenes participate in cell transformation and initiation of tumor formation with mutations of the *Ras* gene detected in approximately 30% of human cancers [9–13]. It is known that H-*ras*^{val12} induces autophagy in human colorectal cancer, breast cancer, cervical cancer, and mesenchymal stem cells through the ERK signaling pathway [14–16]. In contrast, it inhibits the autophagic process through activation of the class I phosphoinositide 3-kinase (PI3K) signaling pathway [17] suggesting dual roles of *ras* genes in the autophagic process. It is also known that Ras upregulates the Atg5 gene and activates the Rac1/MKK7/JNK signaling pathway to induce autophagy [18]. In contrast, recently, Ras upregulates Noxa (a BH3 only protein) through the MEK/ERK pathway to promote autophagy by displacing members of the Bcl-2 family from Beclin 1 [16,19]. Altogether, these studies indicate that the mechanisms and signaling pathways of Ras-induced autophagy are complicated and remain obscure.

BNIP3 (Bcl-2/adenovirus E1B 19-kDa–interacting protein 3) is also known to induce autophagy [20–22], but its relationship with Ras in the induction of autophagy has not been reported. BNIP3 is a mitochondrial proapoptotic protein belonging to the Bcl-2 family. It contains a Bcl-2 homology 3 (BH3) domain and a COOH-terminal transmembrane domain [23]. Its proapoptotic activity is distinct from other members of the Bcl-2 family that it is upregulated by the transcription factor hypoxia-inducible factor 1α, which is activated by Ras through the MEK/ERK signaling pathway [24].

In summary, oncogenic Ras is able to trigger tumorigenesis, upregulate BNIP3, and induce autophagy. In this study, we clarified the roles of Ras as well as BNIP3-induced autophagy in tumorigenesis using mouse NIH3T3 and embryo fibroblast cells.

Materials and Methods

Cell Lines

The H-*ras*^{val12} transformant, 7-4 cell, was derived from mouse NIH3T3 fibroblast. MEF-Atg5(+/+)-Ras^{val12} and MEF-Atg5(−/−)-Ras^{val12} cells derived from wild-type mouse embryonic fibroblasts [MEF-Atg5(+/+)] and Atg5 knockout cells [MEF-Atg5(−/−)] were established in our laboratory. MEF-Atg5(+/+) and MEF-Atg5(−/−) cells (simian virus 40 T antigen immortalized) are from Dr N. Mizushima (Tokyo Medical and Dental University, Japan). MEF-Atg5(+/+)-Ras^{val12} and MEF-Atg5(−/−)-Ras^{val12} the same as 7-4 cell harbor an inducible H-*ras*^{val12} oncogene. All the above cell lines were maintained in Dulbecco modified Eagle medium (12100-061; GIBCO, Gaithersburg, MD) with 10% fetal bovine serum (04-001-1A; Biological Industries, Kibbutz Beit Haemek, Israel) and at 37°C in a 5% CO_2 incubator [10].

Immunofluorescent Staining

Cells (1×10^5 per well) were seeded on a slide and cultured with isopropyl-β-D-thiogalactopyranoside (IPTG, 5 mM, I9003; Sigma, Missouri, MO) for 48 hours, then fixed in methanol for 20 minutes. The slide was incubated for 30 minutes in 0.1% Triton X-100 in phosphate-buffered saline. Anti-LC3 polyclonal antibody (AP1802a; Abgent, San Diego, CA), anti–Beclin 1 polyclonal antibody (sc-11427; Santa Cruz, Santa Cruz, CA) and anti–Bcl-2 monoclonal antibody (sc-783; Santa Cruz) were added on the slide and left overnight at 4°C. The fluorescent change of the cells was investigated under either a fluorescent microscope (DP 70; Olympus, Tokyo, Japan) or a confocal microscope (FV-1000; Olympus).

Transmission Electron Microscopy

Cells after IPTG (5 mM) induction were fixed with 2.5% glutaraldehyde in 0.1 M cacodylate buffer containing 4% sucrose, 1 mM $MgCl_2$, and 1 mM $CaCl_2$ and postfixed in 1% osmium tetroxide. Cells were embedded with LR White (14380; Agar Scientific, Stansted, United Kingdom) after dehydration with ethanol. Ultrathin sections were stained with saturated uranyl acetate and lead citrate at room temperature for 1 hour and investigated under a transmission electron microscope (HITACHI-7000, Tokyo, Japan).

Promoter Activity Assay

After transfection of the BNIP3 (pGL3-BNIP3, 0.2 μg) or Ras activity luciferase reporter plasmid (pY2-Luc; containing Ets binding element, 0.2 μg) [25], the cells (1×10^5 per well) cultured in triplicate in 12-well plates were treated with IPTG and incubated at 37°C for various times. The cells were lysed in 100 μl of lysis buffer (E194A; Promega, Madison, WI). The lysate was assayed for both firefly and *Renilla* luciferase activities using the Dual-Glo Luciferase Assay System following the manufacturer's instructions (E1960; Promega), and relative luciferase unit was measured by a luminometer (EG&G Berthold, Wildbad, Germany). Luciferase activity of the firefly luciferase was normalized for equal transfection efficiency based on *Renilla* luciferase activity in each lysate, which was used as the control. The primers used for construction of various deletion mutants of pGL3-BNIP3 were as follows:

BNIP3 forward 5′-CCTAGCTAGCACCCTTCCAACTCTC-TTCCCTCTC-3′
BNIP3 reverse 5′-CCCCAAGCTTGCGCTCTTCTCTCTC-TCTCCAAAC-3′

Western Blot Analysis

The total protein from the cell lysate was collected from the cells after various treatments. For Western blot analysis, a previously described procedure was applied [26]. The following antibodies were

used: monoclonal antibodies for β-actin (A5441; Sigma), LC3 (PM036; MBL, Nagoya, Japan), Pan-Ras (OP22; Calbiochem, San Diego, CA), Pan-Ras^{val12} (OP38; Calbiochem), p62 (PM045; MBL), Beclin 1 (sc-11427; Santa Cruz), BNIP3 (ab38621 and ab10433 for the detection of monomer and dimmer BNIP3, respectively; Abcam, Cambridge, United Kingdom), Bcl-2 (sc-783; Santa Cruz), and Atg5 (ab54033; Abcam).

Flow Cytometry Analysis

Cell viability. Cells were stained with the propidium iodide (PI, 0.04 mg/ml) (P4170; Sigma) followed by flow cytometry analysis.

Cell cycle. Cells were fixed with 70% ethanol and stored at −20°C overnight, followed by staining with cell cycle buffer (PI, 0.04 mg/ml, 0.1% Triton-X 100 and RNase) followed by flow cytometry analysis.

Cell Transfection and RNA Interference

Cells (2×10^5 per well) in a six-well plate were transfected with 4 μg of pFlag-BNIP3, pHA-Atg5 (a gift from Dr N. Mizushima), pshRNA-Atg5 (Institute of Molecular Biology, Academia Sinica, Taipei, Taiwan), small interfering RNA (siRNA)–negative control (12935-300; Invitrogen, Boston, MA) or siRNA-BNIP3 ([RNA]-GCC CAG CAU GAA UCU GGA CGA AGU A; Invitrogen) by Lipofectamine 2000 following the manufacturer's instructions (Invitrogen). The control vector was pFlag-CMV2 (Invitrogen).

Immunoprecipitation

Cells were harvested in lysis buffer, and 1 mg of cellular protein was incubated with specific antibodies at 4°C overnight. Protein G agarose bead (50 μl; 17-0618-01; GE Healthcare, Amersham, Buckinghamshire, United Kingdom) was mixed with the immunocomplexes and collected after centrifugation by adding SDS-PAGE sample buffer and boiled for 10 minutes. Western blot analysis was conducted and followed by reaction with anti–Bcl-2 or anti–Beclin 1 antibodies. Western blots were incubated with ECL (WBKLS0500; Millipore, Billerica, MA) and exposed it by BioSpectrum AC (101-206-009; UVP, Upland, CA).

MTT Assay

Cells (4×10^3 per well) in the 96-well plates received different treatments for 24, 48, and 72 hours. MTT solution (M2128; Sigma) (0.05 mg/ml in Dulbecco modified Eagle medium) was added to each well at 37°C for 3 hours. The medium was removed, and 100 μl of dimethylsulfoxide (D4540; Sigma) was added. Cell proliferation was determined by measuring the cell lysate at the optical density of 540 nm wavelength using a 96-well multiscanner autoreader (MRX II; Thermo Lab Systems, Franklin, MA).

BrdU Incorporation Assay

Cells (1×10^5 per well) were seeded in six-well trays and treated with IPTG for 48 hours. The cells were grown in bromodeoxyuridine (BrdU; 0.04 mg/ml; B5002; Sigma) containing medium for 30 minutes, fixed in acidic ethanol at −20°C for 10 minutes, and then incubated in 2N HCl for 10 minutes. Anti-BrdU polyclonal antibody (RPN202; GE Healthcare) at a dilution of 1:400 was added to the well overnight at 4°C. The primary antibody was detected by fluorescein isothiocyanate–conjugated goat anti-mouse IgG under a fluorescent microscope (DP 70; Olympus).

Mice and Tumors

Female, 6-week-old NOD/SCID mice were obtained from the Laboratory Animal Center of National Cheng Kung University. The animals were maintained in a pathogen-free facility under isothermal conditions with regular photoperiods. The experimental protocol adhered to the regulation of the Animal Protection Act of Taiwan and was approved by the Laboratory Animal Care and Use Committee of the university. Six-week-old female NOD/SCID mice were injected subcutaneously with 5×10^5 cells in 100 μl of phosphate-buffered saline. Tumor volume was measured according to the formula: $V = 0.52 \times a^2 \times b$ (a indicating the smallest superficial diameter; b, the largest superficial diameter) [27].

Immunohistochemical Staining

Slides of paraffin sections treated with polyclonal anti-LC3 (AP1802a; Abgent) or monoclonal anti-Ki67 antibody (no. RM9106; Thermo Scientific, Santa Clara, CA) were processed as described elsewhere [28]. Briefly, the slides were labeled with biotin-linked secondary antibody followed by streptavidin (K3461; Dako Cytomation, Carpinteria, CA) treatment for 10 minutes at room temperature. The slides were treated with AEC solution for 10 minutes at room temperature and then counterstained with 10% hematoxylin (3000-2; Muto Pure Chemicals Co, Ltd, Tokyo, Japan) and mounted by glycerol gelatin (GG1; Sigma).

Tumor Tissues

Samples were obtained from four patients diagnosed with bladder cancers from Department of Urology, Chia-Yi Christian Hospital, Chia-Yi, Taiwan. Informed consent was obtained from the patients with approval by the institutional review board. Specimens were obtained immediately after surgery and stored at −80°C. The frozen tissue was extracted and homogenized in lysis buffer (the same buffer used for cell lysis). After sonication for 20 minutes, samples were centrifuged at 15,000 rpm for 20 minutes and heated at 100°C for 10 minutes. The RNA was extracted using a single-step method with TRIzol reagent (15596-026; Invitrogen). For reverse transcription–polymerase chain reaction (RT-PCR), first-stand complementary DNA was synthesized 1 μg of total RNA with an oligo-dT primer and the Molony murine leukemia virus reverse transcriptase (M1701; Promega). The sequences of PCR primers were as follows:

BNIP3 forward 5′-GCATGAGTCTGGACGGAGTAG-3′
BNIP3 reverse 5′-CCGACTTGACCAATCCCATA-3′
LC3 forward 5′-CCACACCCAAAGTCCTCACT-3′
LC3 reverse 5′-CACTGCTGCTTTCCGTAACA-3′
β-actin forward 5′-TGGAATCCTGTGGCATCCATGAAAC-3′
β-actin reverse 5′-TAAAACGCAGCTCAGTAACAGTCCG-3′

The PCR protocol was conducted with the BNIP3 and LC3 primers at 94°C for 30 seconds, 60°C for 1 minute, and 72°C for 1 minute (30 cycles), followed by 72°C for 10 minutes. The PCR protocol was performed with the β-actin primer at 94°C for 30 seconds, 55°C for 30 seconds, and 72°C for 1 minute (25 cycles), followed by 72°C for 10 minutes.

Statistical Analysis

All data are presented as the mean ± SD. Differences between the experimental and control groups were analyzed by Student's t test. $P < .05$ was considered statically significant: $^*P < .05$, $^{**}P < .01$, and $^{***}P < .001$.

Results

H-ras^{val12} Induces a Dynamic, Multistep Autophagic Process

We previously established various NIH3T3 stable cell lines harboring the inducible H-*ras*^{val12} oncogene under the regulation of a *lac*-inducible system (designated 7-4 and 2-12) and IPTG has been used to induce H-*ras*^{val12} overexpression. We also demonstrated that H-*ras*^{val12} induces the transformation of NIH3T3 cells [9,26]. The expression of LC3-II, a marker of autophagosomes, was gradually increased from 24 to 48 hours and declined at 72 hours after IPTG induction in 7-4 cells (Figure 1*A*) but not in the parental NIH3T3 cells (Figure W1*A*). The protein expression levels of another two autophagy-related genes, namely, *p62* and *Beclin 1*, were also increased by H-*ras*^{val12} either at 24 or at 48 hours after IPTG induction (Figure 1*A*). These autophagic phenomena were also detected in another inducible H-*ras*^{val12} clone 2-12 cells (data not shown). The double-membrane vesicles with engulfed organelles (autophagosomes, Figure W1*Ba*) as well as the single-membrane vesicles with or without organelles (autophagolysosome-like, Figure W1*Bb*) were detected in 7-4 but not in parental NIH3T3 cells at 48 and 60 hours after IPTG induction under the transmission electron microscope (Figure W1*B*). Our data suggest that H-*ras*^{val12} overexpression triggers autophagy.

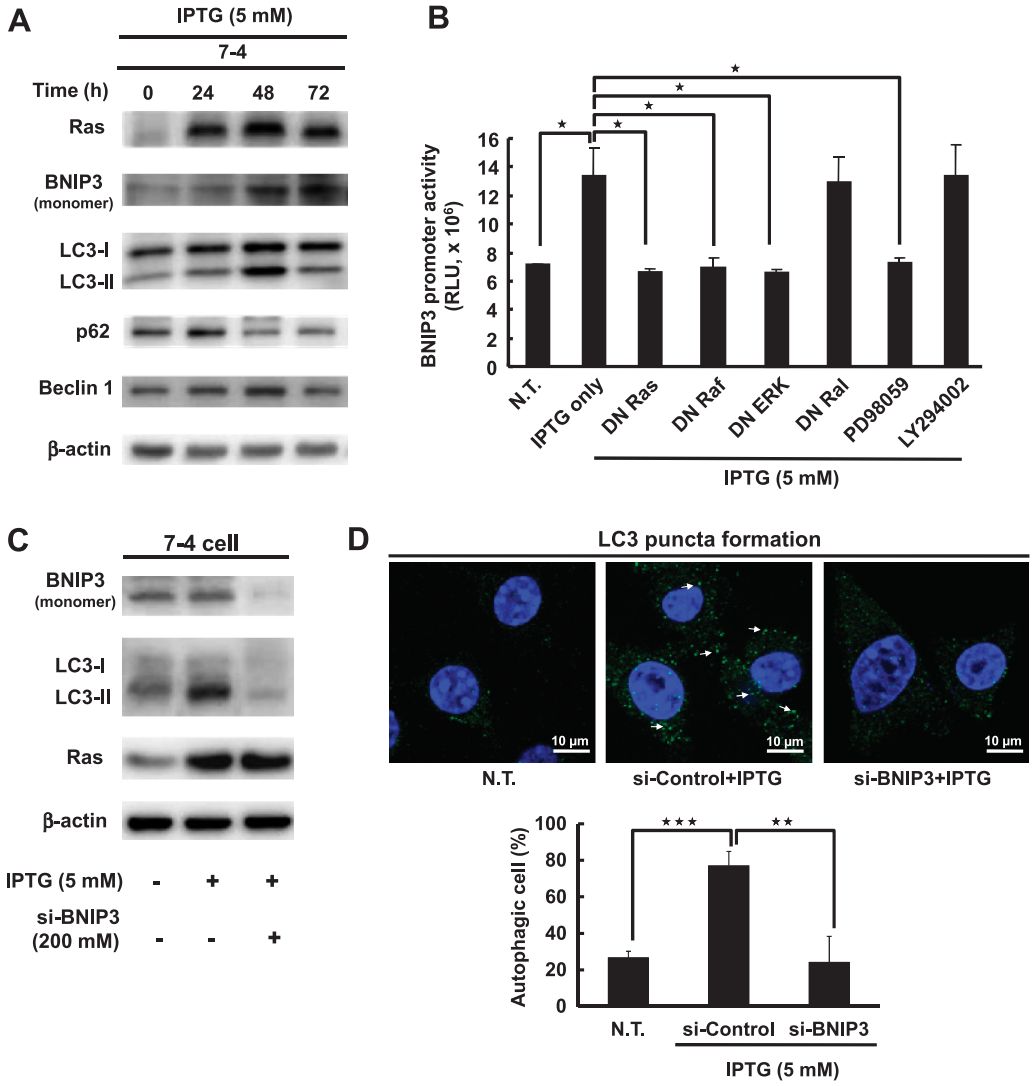

Figure 1. BNIP3 regulates H-*ras*^{val12}–induced autophagy. (A) The 7-4 cells were treated with IPTG for different periods. Total protein extracts and the expression levels of Ras, BNIP3, LC3, p62, and Beclin-1 were evaluated by Western blot analysis using specific antibodies. β-Actin was used as an internal control. (B) The 7-4 cells in the presence of IPTG were cotransfected with BNIP3 reporter plasmid pGL3-BNIP3 together with various DN gene plasmids (DN Ras, DN Raf, DN ERK, and DN Ral) and treated with MEK inhibitor (PD98059) and PI3K inhibitor (LY294002) for 24 hours after transfection. The BNIP3 promoter activity of each group was measured by the Dual-Glo luciferase assay system. NT indicates the cells without any treatment. This experiment was conducted in triplicate and repeated at least three times. (C) The 7-4 cells were transfected with BNIP3 siRNA (200 mM) and RNAi-negative control (200 mM) for 48 hours by Lipofectamine 2000. The expression levels of BNIP3, LC3, and Ras protein were measured by Western blot analysis. (D) The 7-4 cells were transfected with BNIP3 siRNA (200 mM) and RNAi-negative control (200 mM) for 48 hours, and LC3 puncta were investigated under a confocal fluorescent microscope with anti-LC3 antibody and detected by fluorescein isothiocyanate–conjugated goat anti-rabbit IgG. NT indicates the cells without any treatment. Cells containing 30 or more green LC3 puncta were defined as autophagic cells. Thirty cells were evaluated by field, and three fields were counted. Error bars represent SD. *$P < .05$, **$P < .01$, or ***$P < .001$. Student's *t* test.

To further clarify that H-*ras*^{val12} induced autophagic flux and caused the degradation of LC3-II and p62 at 72 hours after induction, we used chloroquine (CQ), a blocker of autophagosome and lysosome fusion, was used. Without CQ treatment, 7-4 cells showed very low level of LC3-II expression at 72 hours after IPTG induction (Figures 1*A* and W2*A*, *lane 2*) or without IPTG induction (Figure W2*A*, *lane 1*). When the cells at 48 hours after IPTG induction were treated with CQ for another 24 hours, evident accumulation of LC3-II and p62 protein was detected (Figure W2*A*, *lane 3*), indicating that an autophagic flux was induced. To confirm that H-*ras*^{val12} overexpression indeed induced the autophagic flux, a tandem fluorescent-tagged LC3 (mRFP-GFP) reporter plasmid (ptfLC3) was transfected into 7-4 cells. The mRFP-LC3 is resistant to acidic conditions and continues to expression both before and after fusion with lysosomes, but GFP expression was quenched because of acidic conditions in the lysosome. Collectively, in the cell, yellow-colored LC3 puncta represent the steady-state autophagosome formation and red coloring represents the autophagy progression from autophagosome to autolysosome, a sign of autophagic flux [29]. Our data show that abundant red fluorescence (RFP) was detected at 72 hours after IPTG induction compared with the cells without induction (Figure W2*B*, NT *vs* IPTG). Furthermore, under the condition of IPTG induction, yellow fluorescence became predominant in the cells when CQ was added at 48 hours after induction to block the fusion of autophagosome and lysosome (Figure W2*B*, IPTG *vs* IPTG + CQ). Altogether, our Western blot analysis and fluorescent image data demonstrate that H-*ras*^{val12} overexpression *per se* induces an autophagic flux in NIH3T3 cells.

*BNIP3 and Raf-1/ERK Signaling Pathway Are Required for H-*ras^{val12}*–Induced Autophagy*

That H-*ras*^{val12} upregulates BNIP3 gene expression has been reported by a microarray analysis [30]. BNIP3 protein expression, both of monomer and dimmer, were gradually induced by H-*ras*^{val12} 24 to 72 hours after IPTG induction (Figure 1*A*, monomer and Figure W3). To clarify how H-*ras*^{val12} oncogene regulates BNIP3 expression, a BNIP3 luciferase promoter plasmid (pGL3-BNIP3) was constructed and transiently transfected into 7-4 cells. The BNIP3 promoter activity was induced about two-folds when IPTG treatment for 48 hours compared with 0 hour of treatment (Figure W4). The plasmid pY2-Luc containing multiple Ets binding elements in the promoter was used as an indicator of Ras activation [25] (Figure W4). It indicates that H-*ras*^{val12} upregulates BNIP3 at the transcriptional level. Further study showed that the dominant-negative (DN) plasmids of Ras (DN-Ras), Raf-1 (DN-Raf), ERK (DN-ERK), and the MEK inhibitor PD98059 significantly suppressed BNIP3 promoter activity ($P < .05$). In contrast, DN RalGDS (DN-Ral) and the PI3K inhibitor LY294002 had no effect on BNIP3 promoter activity (Figure 1*B*). In summary, H-*ras*^{val12} upregulates BNIP3 at transcriptional level through the Raf-1/ERK signaling pathway.

Activation of the Raf-1/ERK pathway by H-*ras*^{val12} overexpression and induction of autophagy was confirmed by the pharmaceutical inhibitor U0126 (an inhibitor of MEK1 and MEK2), which suppressed the phosphorylation level of ERK (p-ERK1/2) and decreased the expression level of LC3-II in a dosage-dependent manner (Figure W5*A*). It is consistent with some reports that H-*ras*^{val12} induces autophagy through ERK pathway [14,15]. Furthermore, LC3-II expression was almost undetectable in the 7-4 derivatives Ras-1 cells (containing H-*ras*^{val12} and DN *ras*^{Asn17} plasmids) and Raf-M cells (H-*ras*^{val12} and DN *raf-1*^{4B} plasmids) [10] under H-*ras*^{val12} overexpression conditions at 24 and 48 hours after induction (Figure W5*B*). It is indicated that H-*ras*^{val12} induces autophagy through the Raf-1/ERK signaling pathway. To clarify whether BNIP3 participates in H-*ras*^{val12}–induced autophagy through the Raf-1/ERK signaling pathway, siRNA of BNIP3 was used. LC3-II expression and LC3 puncta were decreased when H-*ras*^{val12}–induced BNIP3 was suppressed by BNIP3 siRNA (Figure 1, *C* and 1*D*). These data indicate that H-*ras*^{val12} induces autophagy in a BNIP3-dependent manner. Altogether, H-*ras*^{val12} activated BNIP3 through the Raf-1/ERK signaling pathway. Both BNIP3 and the Raf-1/ERK are required for H-*ras*^{val12}–induced autophagic machinery.

*H-*ras^{val12}*–Induced BNIP3 Triggers the Release of Beclin 1 from the Beclin 1–Bcl-2 Complex*

It is known that BNIP3 induces autophagy under hypoxic conditions by competing with Beclin 1 for Bcl-2 [31,32]. To clarify whether H-*ras*^{val12}–induced autophagy also works through the same mechanism, the relationship among BNIP3, Beclin 1, Bcl-2, and autophagy was investigated. In the cells from 24 to 72 hours after IPTG induction, the binding between Bcl-2 and Beclin 1 was dramatically decreased at 48 hours demonstrated by immunoprecipitation (Figure 2*A*, fold change from 1 to 0.6). At the same time point, colocalization of Beclin 1 and Bcl-2 (yellow dots) was decreased by immunofluorescent staining (Figure 2*B*; NT *vs* IPTG). Our result show that the greatest loss of the association between Bcl-2 and Beclin 1 was at 48 hours after IPTG induction (Figure 2*A*). However, only part of Beclin 1 was displaced by BNIP3, so the Beclin 1–Bcl-2 complex is still detectable but at a reduced level at 72 hours under *ras* overexpression conditions. These results suggest the increase of Beclin 1 release from the Beclin 1–Bcl-2 complex, whereas H-*ras*^{val12} was overexpressed. The relationship among BNIP3, Bcl-2, and Beclin 1 was further confirmed either by overexpression of ectopic BNIP3 (pFlag-BNIP3), which decreased colocalization of Beclin 1 and Bcl-2 ($P < .01$), or by silencing BNIP3 expression (siBNIP3), which increased the binding of Beclin 1 to Bcl-2 ($P < .05$) (Figure W6). Taken together, our results suggest that the binding between Beclin 1 and Bcl-2 is partially affected by BNIP3 competition. In summary, H-*ras*^{val12}–induced BNIP3 expression triggers autophagy possible through the increase of Beclin 1 release from the Beclin 1–Bcl-2 complex.

Mutant Ras^{val12} Together with BNIP3 and LC3-II Overexpression Are Detected in the Tumor Parts of Clinical Bladder Cancer Specimens

To elucidate whether H-*ras*^{val12} upregulating BNIP3 and inducing autophagy occur in human cancers, eight paired bladder cancer specimens (normal part [N] and tumor [T]) were analyzed. Overexpression of mutant *Ras*^{v}, BNIP3, and LC3-II protein was detected in the tumor parts of 75% bladder cancer specimens (6/8) (Figure 3*A*). Consistently, the tumor specimens showing higher expression of BNIP3 and LC3 protein also expressed higher level of mRNA detected by RT PCR (Figure 3*B*). This result is consistent with our above *in vitro* experiments shown in Figure 1*B* and Figure W4 showing that Ras regulates BNIP3 and autophagy at the transcriptional level. Altogether, mutant Ras together with BNIP3 overexpression and autophagy activation positively correlates with tumorigenesis of bladder cancer.

*H-*ras^{val12}*–Induced Autophagy Suppresses Cell Proliferation and Causes Cell Cycle Arrest*

To determine the effect of H-*ras*^{val12} induced autophagy on cell fate, cell proliferation was evaluated after IPTG induction. Our data show that under normal serum (10%) conditions, cell number was

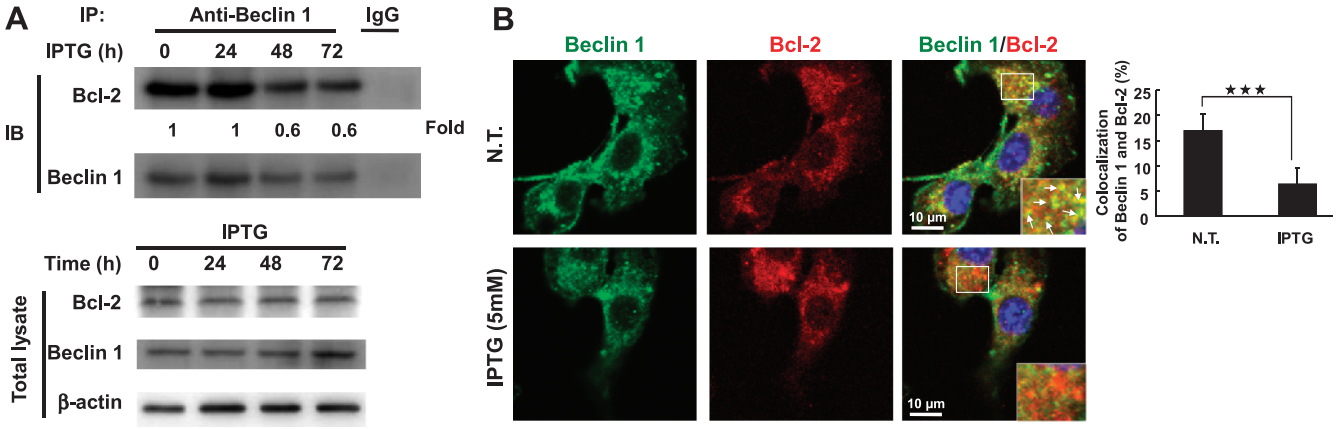

Figure 2. H-*ras*^{val12}–induced BNIP3 triggers the release of Beclin 1 from Beclin 1–Bcl-2 complex. (A) The 7-4 cells after IPTG treatment for 24, 48, and 72 hours; the total protein extract was immunoprecipitated by anti–Beclin 1 antibodies and followed by immunoblot analysis to evaluate the levels of Bcl-2 and Beclin 1. (B) With or without IPTG treatment of 7-4 cells for 48 hours, the decreased colocalization of Beclin 1 (green) and Bcl-2 (red) was assessed under a fluorescence microscope. The white arrow points the colocalization of Bcl-2 and Beclin 1 (yellow spots). The percentage of colocalization of Beclin 1 and Bcl-2 was quantified by counting the yellow dots in the cell. Error bars represent SD. ***$P < .001$. Student's *t* test.

significantly decreased after H-*ras*^{val12} overexpression for 48 and 72 hours (compared to the cells without IPTG induction) demonstrated by MTT assay (Figure 4*A*). To clarify that the decreased cell number was caused by increased cell death or decreased cell proliferation, flow cytometry was used to evaluate cell viability, and BrdU incorporation was conducted to determine cell proliferation. H-*ras*^{val12} overexpression does not affect cell viability from 0 to 120 hours after IPTG induction as demonstrated by flow cytometry analysis (Figure 4*B*). Prabhakaran

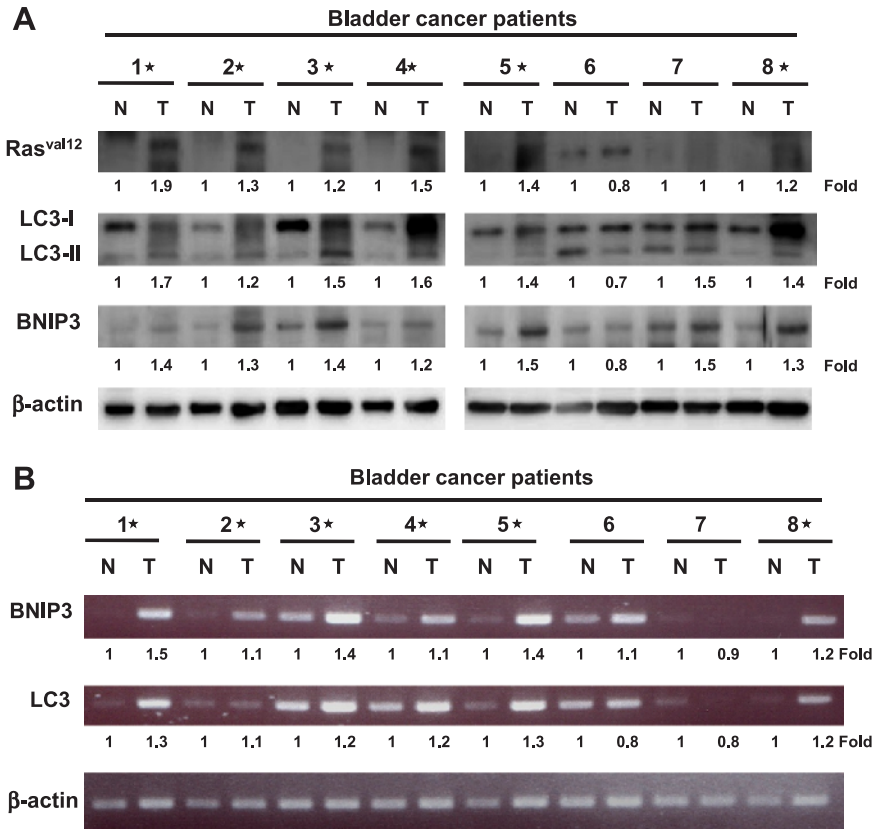

Figure 3. Mutant Ras^{val12} together with BNIP3 and LC3-II overexpression is detected in the tumor parts of the bladder cancer specimens. (A) Immunoblot analysis of eight paired human bladder cancer specimens (tumor [T] and adjacent normal tissue [N]) for Pan-Ras^{val12}, LC3, and BNIP3 protein expression using specific antibodies. (B) The RNA of the above specimens was extracted for BNIP3 and LC3 expression by RT-PCR analysis. *Overexpression of Ras^{val12}, BNIP3, and LC3-II of the protein (A) and RNA (B) comparing the tumor *versus* normal tissue.

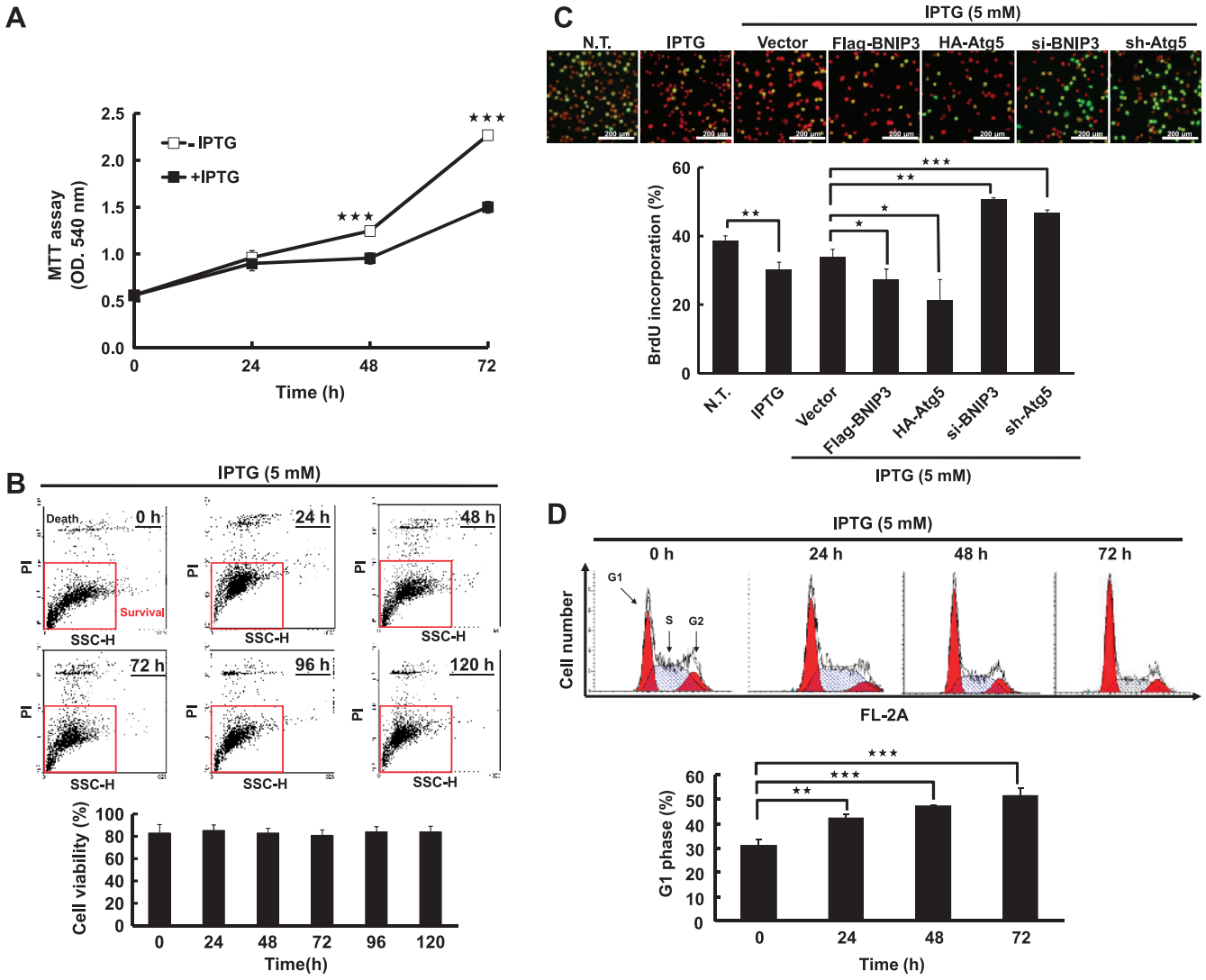

Figure 4. Autophagy suppresses H-*ras*^{val12}–induced cell proliferation. (A) The 7-4 cells were treated with or without IPTG for 24, 48, and 72 hours. Cell growth was measured by MTT assay. (B) The 7-4 cells were treated with IPTG (5 mM) for 24, 48, 72, 96, and 120 hours and followed by PI (0.04 mg/ml) labeling. Cell viability was evaluated by flow cytometry analysis, and cell population and quantitative data were shown. (C) The 7-4 cells in the presence of IPTG were transfected with plasmids pFlag-BNIP3 (4 μg), pHA-Atg5 (4 μg), psh-Atg5 (4 μg), si-BNIP3 (200 mM), or pFlag-CMV2 (Vector) for 48 hours. Cell proliferation was determined by BrdU (0.02 g/ml) incorporation for 30 minutes. Anti-BrdU antibody and PI were used to label the treated cells for cell proliferation and nuclei, respectively. The merged images showing green or yellow fluorescent cells represent proliferating cells, which were used to quantify the percentage of cell proliferation. (D) The 7-4 cells were treated with IPTG for various times, and cell cycle was analyzed by PI staining followed by flow cytometry analysis. (E) The MEF-Atg5(+/+)-Ras^{val12} and MEF-Atg5(−/−)-Ras^{val12} cells with or without IPTG treatment for 48 hours. Cell proliferation was measured by BrdU staining. This experiment was conducted in triplicate and was repeated for three times. (F) The 7-4 cells received two different treatments: 1) Short-time IPTG induction. The 7-4 cells were transfected with plasmid pHA-Atg5, psh-Atg5, or pHA-CMV (vector) for 48 hours followed by IPTG induction for another 48 hours. 2) Long-time IPTG induction. The 7-4 cells were treated IPTG for 14 days and in the presence of IPTG followed by transfection with pHA-Atg5, psh-Atg5, or pHA-CMV plasmids for 48 hours. Cell proliferation was measured by MTT assay. (G) The 7-4 cells received the same treatment as in F were analyzed by BrdU incorporation assay for cell proliferation. Error bars represent SD. *$P < .05$, **$P < .01$, or ***$P < .001$. Student's t test)

et al. [33] and Quinsay et al. [34] reported that BNIP3 induces cell death together with loss of mitochondrial membrane potential ($\Delta\Psi_m$). Differently, in our study, H-*ras*^{val12} overexpression did not decrease mitochondrial membrane potential ($\Delta\Psi_m$) from 0 to 120 hours after induction (Figure W7). In summary, our data indicate that the increase of BNIP3 does not induce cell death when H-*ras*^{val12} is overexpressed.

To further clarify cell proliferation was suppressed by H-*ras*^{val12} overexpression and H-*ras*^{val12}–induced autophagy, *BNIP3* and *Atg5* (an essential gene for canonical autophagy) genes were manipulated in 7-4 cells to control autophagic activity. Briefly, *BNIP3* and *Atg5* genes were overexpressed or silenced in 7-4 cells by pFlag-BNIP3 or pHa-Atg5 to enhance autophagic activity and by siBNIP3 or shAtg5 RNA to suppress autophagic activity. Our data show that cell proliferation was inversely correlated with autophagic activity demonstrated by BrdU incorporation assay (Figure 4*C*). In 7-4 cells, overexpressing or silencing *BNIP3* and *Atg5* indeed affected autophagic activity as was demonstrated by the LC3-II expression level and immunofluorescent staining (Figures 1, *C* and *D*, and W8). Furthermore, cell cycle was

analyzed by flow cytometry, whereas H-*ras*^{val12} was overexpressed and the increased accumulation of cell population at the G_0/G_1 phase from 24 to 72 hours was detected (Figure 4*D*; 30%-53%), indicating cell cycle arrest at the G_1 phase. To further clarify cell proliferation suppressed by H-*ras*^{val12} overexpression–induced autophagy, wild-type mouse embryo fibroblast and *Atg5* knockout MEF cell lines harboring the inducible H-*ras*^{val12} were established. They are designated as MEF-Atg5(+/+)-Ras^{val12} and MEF-Atg5(−/−)-Ras^{val12}, respectively. Because MEF-Atg5(−/−) is an autophagy-deficient cell line, the expression of LC3-II induced by Ras and accompanied with *Atg5* expression was detected only in MEF-Atg5(+/+)-Ras^{val12} but not in MEF-Atg5(−/−)-Ras^{val12} cells (Figure W9). H-*ras*^{val12} overexpression suppressed MEF-Atg5(+/+)-Ras^{val12} cell proliferation but not MEF-Atg5(−/−)-Ras^{val12} cells (Figure 4*E*), further supporting the results mentioned above. In summary, we propose that autophagy suppresses cell proliferation through cell cycle arrest at the G_1 phase under H-*ras*^{val12} overexpression conditions. To clarify the temporal role of H-*ras*^{val12}–induced autophagy in cell proliferation, pHa-Atg5 plasmid DNA and shAtg5 RNA were used to enhance or suppress H-*ras*^{val12}–induced autophagy, respectively. Our data show that within 48 hours, overexpression of ectopic Atg5 was followed by H-*ras*^{val12} overexpression (short-time *ras*^{val12} overexpression); autophagy plays a suppressive role in cell proliferation. However, overexpression of ectopic Atg5 after constitutive Ras overexpression in 7-4 cells for 2 weeks (long-time *ras*^{val12} overexpression), autophagy switches to a promoting role in cell proliferation demonstrated by MTT and BrdU analysis (Figure 4, *F* and *G*). The above event was reversed when autophagy was suppressed by sh-Atg5. Altogether, H-*ras*^{val12}–induced autophagy temporally regulates cell proliferation.

H-ras^{val12}–Related Tumorigenesis Is Suppressed When Autophagy Activity Is Ectopically Induced

The data presented here demonstrate that increased autophagy followed by H-*ras*^{val12} overexpression suppressed cell proliferation. To further confirm whether autophagy plays a suppressive role in tumor formation, MEF-Atg5(+/+)-Ras^{val12} and MEF-Atg5(−/−)-Ras^{val12} cells' tumor formation in the mouse model was conducted. Our data show that both mouse MEF-Atg5(+/+)-Ras^{val12} and MEF-Atg5(−/−)-Ras^{val12} cells were able to form tumors when they were injected subcutaneously (s.c.) into NOD/SCID mice. Comparing the tumor size induced by these two cell lines regardless with or without IPTG induction, the tumor weight of the MEF-Atg5(−/−)-Ras^{val12} group in the presence of IPTG is the largest (Figure 5*A*). Tumor size induced by MEF-Atg5(−/−)-Ras^{val12} was decreased by the expression of HA-tagged Atg5 protein (Figure 5*B*), indicating that autophagy plays a suppressive role in H-*ras*^{val12}–induced tumor formation.

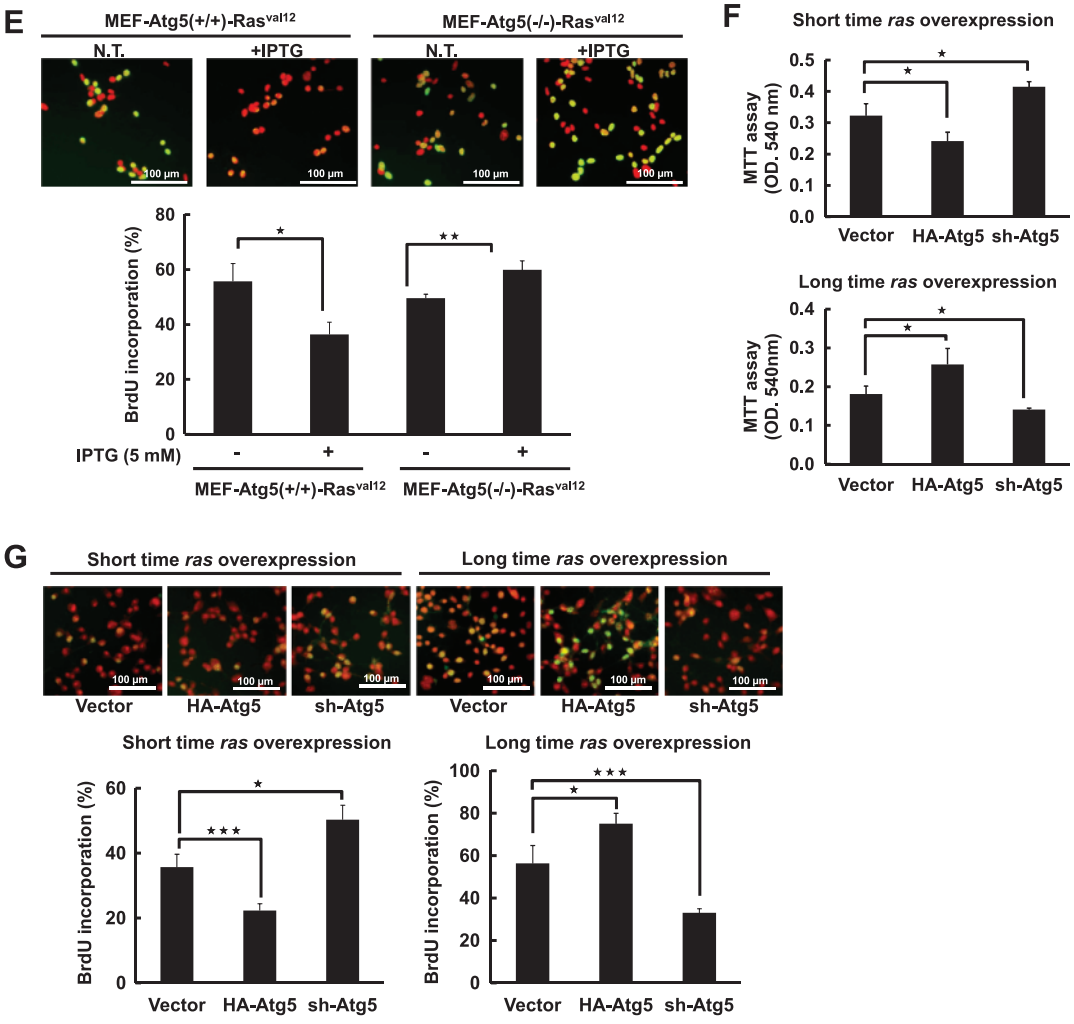

Figure 4. (*continued*).

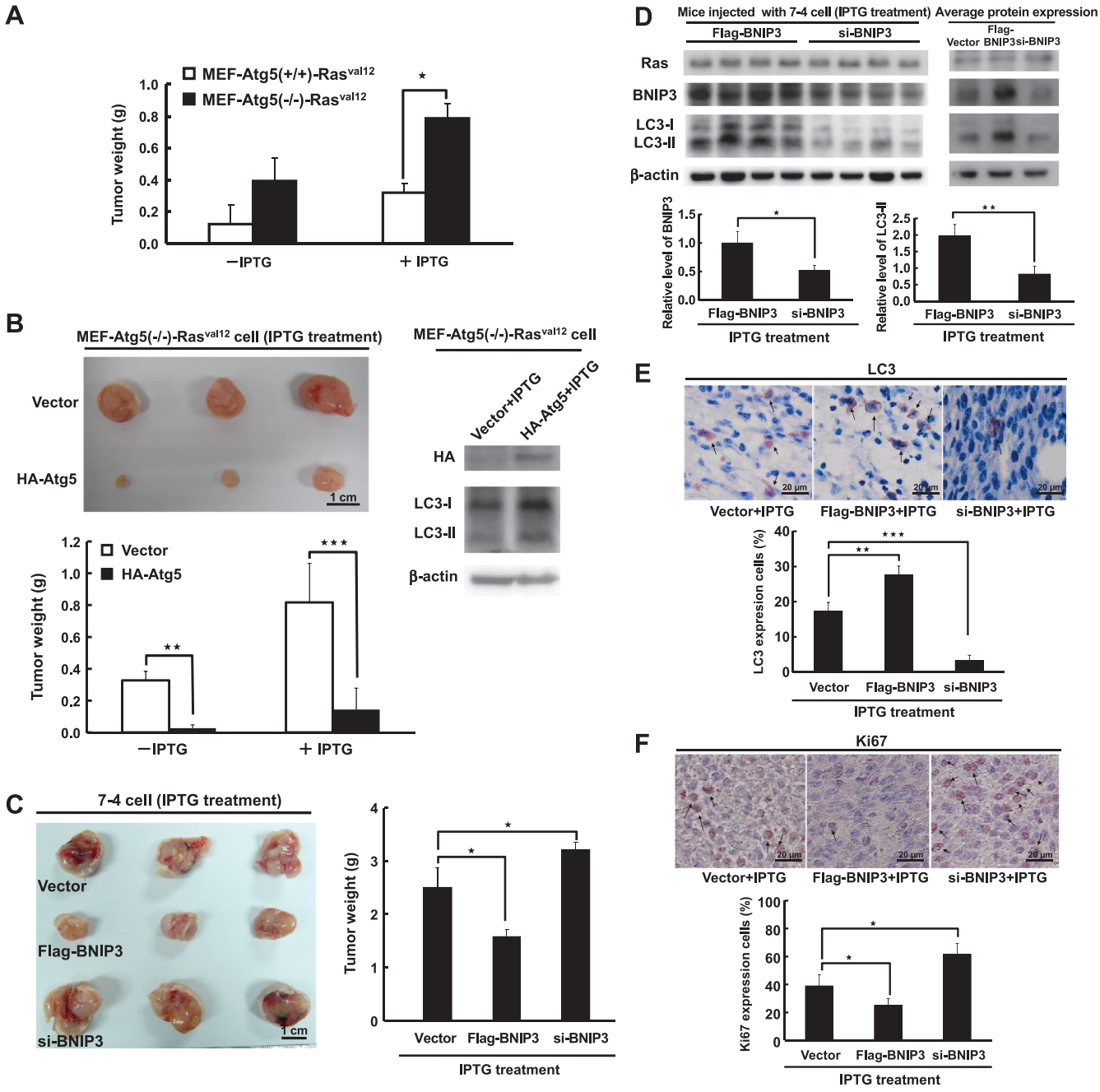

Figure 5. Autophagy inhibits cell proliferation to suppress Ras-induced tumor formation. (A) The MEF-Atg5(+/+)-Ras^{val12} and MEF-Atg5(−/−)-Ras^{val12} cells (5×10^5) with or without IPTG treatment were injected s.c. into SCID mice. The tumor weight was measured at 14 days after IPTG induction. (B) The MEF-Atg5(−/−)-Ras^{val12} cells with or without IPTG treatment were transfected with HA-Atg5 (pHA-Atg5; 4 μg) or vector (pHA-CMV) for 48 hours. The cells (5×10^5) were injected s.c. into SCID mice. Each group composed of three mice. The tumor weight was measured at 13 days after IPTG induction. (C) The 7-4 cells (1×10^6/well) after transfection of BNIP3 siRNA (200 mM), pFlag-BNIP3, or vector control plasmid DNA (24 μg) for 48 hours in the presence of IPTG were injected into the left and right sides of each mouse. Mice were fed with IPTG (12.5 mM) containing water for 15 days. (D) Protein extracted from the tumors of the killed mice was analyzed by immunoblot analysis for Ras, LC3, and BNIP3 protein expression. There were four mice in each group. Left panel shows the protein expression of each of the four treated mice; the right panel represents the average protein expression of four mice protein mixture. (E) The sections from the tumors were labeled with rabbit-conjugated LC3 antibody for LC3 expression. The arrows point at the LC3 expressing cells. (F) Representative sections of the tumors were labeled with anti-Ki67 antibody to detect Ki67 expression. The arrows point at the Ki67-positive cells. Error bars represent SD. *$P < .05$, **$P < .01$, or ***$P < .001$. Student's t test.

We previously demonstrated that mouse NIH3T3 cells over-expressing H-*ras*^{val12} form tumors in NOD/SCID and BALB/c mice [9]. To further clarify the suppressive effect of autophagy on tumorigenesis, the NIH3T3 derivate 7-4 cell together with ectopic BNIP3 or BNIP3 siRNA for 48 hours followed by H-*ras*^{val12} overexpression was s.c. injected into the mice. Similar to the results of MEF-Atg5(−/−)-Ras^{val12} cells in Figure 5, *A* and *B*, overexpression of flag-tagged BNIP3 in 7-4 cells decreased tumor weight and decreased BNIP3

expression by siRNA-increased H-*ras*^{val12}–related tumor formation (Figure 5*C*). The expression levels of BNIP3 and LC3-II were indeed higher in tumors of 7-4 cells expressing the ectopic *BNIP3* gene. Conversely, the expression levels of BNIP3 and LC3-II were low in the tumors treated with BNIP3 siRNA (Figure 5*D*, *left panel*: the protein expression of each of the four treated mice; *right panel*: the average protein expression of four mice protein mixture). Furthermore, the expression level of LC3 protein in tumor tissue detected by immunohistochemical staining (Figure 5*E*) is consistent with the result of Western blot analysis (Figure 5*D*). Our data demonstrate that H-*ras*^{val12} induces autophagic activity and tumorigenesis simultaneously, and overexpression of ectopic BNIP3 increases autophagic activity in tumors. In contrast, silencing endogenous BNIP3 reduced autophagic activity. In addition, Ras expression levels in all of the tumors were similar (Figure 5*D*), suggesting that *ras* is required for tumor formation but is dispensable for the influence on tumor size through BNIP3 regulation of autophagic activity.

Autophagy has been shown to exert an inhibitory effect on tumor formation through induction of cell death [5,16]. However, in our inducible system, H-*ras*^{val12} BNIP3–induced autophagy did not cause cell death before 48 hours, which was confirmed by autophagy inducer rapamycin, overexpression of BNIP3, Atg5, or by suppression of autophagy with shAtg5 or siBNIP3 (Figure W10). To clarify whether suppression of H-*ras*^{val12}–induced tumor formation by BNIP3-mediated autophagy is through inhibition of cell proliferation, Ki67 (an indicator of cell proliferation) was used to stain the tumor sections collected from the above tumor formation experiment (Figure 5*F*). Our data show that tumor cell proliferation in the presence of IPTG was significantly increased when BNIP3 expression was silenced by siRNA compared with the tumor cells overexpressing ectopic BNIP3 or vector control (Figure 5*F*). This result is consistent with the above the data of our *in vitro* study, which showed that H-*ras*^{val12}–related autophagy inhibits cell proliferation (Figure 4*C*). Taken together, H-*ras*^{val12}–induced tumor formation of the NIH3T3 cells in mice can be suppressed by BNIP3-induced autophagy through inhibition of cell proliferation. In conclusion, H-*ras*^{val12} induces BNIP3 overexpression, autophagy, and tumorigenesis simultaneously. When BNIP3 expression is further boosted, induced autophagy plays a suppressive role in regulating H-*ras*^{val12}–related cell transformation and tumorigenesis.

Discussion

In this study, we revealed that H-*ras*^{val12} oncogene upregulates BNIP3 at the transcriptional level through the Raf-1/MEK/ERK signaling pathway. Our finding that Raf-1/MEK/ERK is the major signaling pathway for H-*ras*^{val12}–induced autophagy (Figure W5) is consistent with reports from the human mesenchymal stem cells and HT-29 cells [14,15]. Byun et al. [18] reported that H-*ras*^{val12} increases Atg5 expression and activates the Rac1/MKK7/JNK signaling pathway to induce autophagic cell death. This indicates that H-*ras*^{val12} may use diverse signaling pathways to induce autophagy as well as autophagic responses depending on the stimuli encountered and the cell types. Furthermore, GAIP (a mammalian GTPase activating protein) and NOXA (a BH3-only protein) are downstream mediators of the MEK/ERK signaling pathway to induce autophagy in colon cancer HT-29 cells and breast cancer MCF-7 cells, respectively [15,16]. Here, we reveal that BNIP3 is another downstream molecule of the MEK/ERK signaling pathway to induce autophagy in mouse fibroblast cells. Consistent with the report of Elgendy et al. [16], we also detected that H-*ras*^{val12} induces autophagic flux *in vitro,* as demonstrated by degradation of LC3-II and p62 protein at the late stage of autophagic progression (Figure 1*A*; 72 hours) as well as the accumulation of LC3-II and p62 after the treatment with CQ at 48 hours after IPTG induction (Figure W2, *A* and *B*).

During hematopoiesis, a stem cell factor binds the receptor, activates hypoxia-inducible factor 1α, and upregulates BNIP3 through the Ras/MEK/ERK and PI3K signaling pathways [24]. Similarly, H-*ras*^{val12} upregulates BNIP3 at a transcriptional level through the Raf-1/MEK/ERK signaling pathway. BNIP3 overexpression induces either apoptosis or autophagy in a cell type–specific manner [23]. Under the conditions of H-*ras*^{val12} overexpression, BNIP3 is upregulated and autophagy is induced in mouse fibroblast cell lines (NIH3T3 and MEF). A similar event was also detected in human bladder cancer T24 cells (which expresses the H-*ras*^{val12} oncogene). BNIP3, a member of Bcl-2 family induced by hypoxia, competes with Beclin 1 for Bcl-2 binding, and Beclin 1 is released to induce autophagy [31,32,35]. Noxa, another Bcl-2 family member and a BH3-only protein, is also upregulated by H-*ras*^{val12} and promotes autophagy by displacing MCL1 (a Bcl-2 family member), from Beclin 1 [16,19]. Similarly, in NIH3T3 cells, BNIP3 induced by H-*ras*^{val12} competes with Bcl-2 for the binding with Beclin 1 (Figures 2, *A* and *B*, and W6). The interaction between Beclin 1 and Bcl-2 is decreased at 48 and 72 hours after IPTG induction as compared with the control (fold change from 1 to 0.6). The greatest loss of the association between Bcl-2 and Beclin 1 was at 48 hours after IPTG induction (Figure 2*A*). BNIP3 competed with Beclin 1 for binding with Bcl-2 under *ras* overexpression conditions. Therefore, the binding between Beclin 1 and Bcl-2 was decreased. However, the Beclin 1–Bcl-2 complex is still detectable but at a reduced level at 72 hours after IPTG induction, indicating that only part of Beclin 1 was displaced by BNIP3. Furthermore, H-*ras*^{val12} overexpression also increases Beclin 1 expression (Figure 1*A*), which also contributes to autophagy induction. In summary, H-*ras*^{val12}–induced BNIP3 expression triggers autophagic progression possibly through the increase of Beclin 1 release from Beclin 1–Bcl-2 complex as well as Beclin 1 expression. Furthermore, whether Ras-induced BNIP3 competes with Beclin 1 on the endoplasmic reticulum or on mitochondria requires further investigation. BNIP3 is a specific activator of mitochondrial autophagy (mitophagy) and the mitochondrial membrane potential ($\Delta\Psi_m$) is decreased in mitophagy mediated by BNIP3-LC3 interaction [21,22]. In this study, H-*ras*^{val12} overexpression did not decrease mitochondrial membrane potential in 7-4 cells (Figure W7); however, the possibility that BNIP3 induces autophagy through BNIP3-LC3 interaction cannot be excluded.

Oncogenic Ras activation without other oncogenic alterations induces autophagy followed by cell death through suppression of the mammalian target of rapamycin (mTOR) signaling pathway [36–38]. However, in tumor cells, Ras-induced autophagy is required to maintain energy balance and prevents cells from death. The reports cited indicate that cell fate affected by Ras-induced autophagy remains contradictory. In this study, Ras overexpression-induced autophagy blocks cell proliferation both *in vitro* and *in vivo* using mouse fibroblast cells. Denoyelle et al. [39] demonstrated that H-*ras*^{val12}-induced senescence is mediated by unfolded proteins associated with the endoplasmic reticulum and is a critical step in tumor suppression. By contrast, oncogenic K-*ras* escapes premature senescence during tumorigenesis of primary pancreatic duct epithelial cells through up-regulation of twist and suppression of p16^{INK4A} [40]. Collectively, *ras* oncogene induces or escapes cell proliferation and senescence depending on other

oncogenic mutations, duration of Ras overexpression, cell types, and microenvironments. In this study, cell death (Figure 4*B*), suppression of mTOR signaling (Figure W11), and cell senescence (Figure W12) were not detected when autophagy was induced by H-*ras*^{val12} in mouse fibroblast cells. Briefly, Figure W11 shows that the phosphorylation of both mTOR and p70S6K was increased, suggesting that mTOR/p70^{S6K} signaling pathway is not involved. Furthermore, Figure W12, *A* and *B*, shows that no β-glactosidase–expressing cells as well as overexpression of DCR2 protein (indicators of cell senescence) were detected. Instead, H-*ras*^{val12}–induced autophagy suppressed cell proliferation (Figure 4*C*) accompanied with cell cycle arrest at the G_0/G_1 phase (Figure 4*D*). Similarly, tumor formation in mice was also suppressed by ectopic expression of BNIP3 through inhibition of cell proliferation, as demonstrated by Ki67 staining in tissue (Figure 5, *C* and *F*). In conclusion, our finding that H-*ras*^{val12}–induced autophagy suppresses tumor formation through suppression of cell proliferation without causing cell death is different from other reports using different cell lines [18,41,42]. H-*ras*^{val12}–induced autophagy suppresses cell proliferation possibly through cell cycle arrest at the G_0/G_1 phase. It is known that autophagy may degrade the ubiquitinated proteins that bind LC3 through p62 [4]. Cell cycle–related protein cyclin D1 is ubiquitinated and degraded by proteasomes during cell cycle progression [43]. So, it is possible that the induced cell cycle arrest at the G_0/G_1 stage by Ras, as well as the suppression of cell proliferation is mediated through the degradation of cyclin D1 by autophagy.

The evidences claiming that autophagy plays either a suppressing or a promoting role in tumorigenesis are accumulating [16,19,44–46]. Our data show that H-*ras*^{val12} simultaneously induces tumor formation and autophagic activity; however, under such conditions, the level of autophagy seems not sufficient to suppress tumorigenesis, indicating that Ras plays a dominant role during tumor formation. By overexpressing ectopic BNIP3 in H-*ras*^{val12}–overexpressing cells, autophagic activity was further boosted and the dominance of H-*ras*^{val12}–induced colony formation (data not shown) as well as tumor formation was subverted (Figure 5*C*). Negative regulation of H-*ras*^{val12}–induced tumor formation by autophagy was further confirmed by using MEF-Atg5(+/+)-Ras^{val12} and MEF-Atg5(−/−)-Ras^{val12} cells (Figure 5, *A* and *B*). In conclusion, tumorigenesis induced by H-*ras*^{val12} is negatively regulated by autophagy when its level is over or under a specific threshold (referred as the "Goldilocks principle") [16,19]. However, in immortalized baby mouse kidney cells or pancreatic ductal adenocarcinoma cells with Ras overexpression, autophagy was induced to promote tumorigenesis. Similarly, in the human bladder cancer cell line T24, autophagy also plays a promoting role in T24 cell proliferation demonstrated by BrdU analysis using siRNA of BNIP3 or Atg5 (Figure W13). In eight bladder cancer patients analyzed, 75% of the specimens showed high expression of mutant Ras^{val12}, BNIP3, and LC3-II proteins as well as the mRNA in the tumor part (Figure 3, *A* and *B*). Collectively, this indicates that autophagy plays a promoting role in bladder cancer tumorigenesis, which is consistent with three recent reports [45–47]. Further study is required to clarify the underlying mechanism of the autophagic responses to the cells overexpressing the Ras oncogene and affecting tumorigenesis.

We have shown that *ras* overexpression–induced autophagy blocks cell proliferation both *in vitro* and *in vivo* using mouse fibroblast cell lines (MEF and NIH3T3). Interestingly, when Ras overexpression in these cells was continued for 2 weeks, the effect of autophagy on cell proliferation switches from suppression to promotion (Figure 4, *F* and *G*), indicating a temporal regulation of autophagy on cell fate. However, the underlying mechanism of the temporal regulation of autophagy on cell fate currently is unclear and requires further investigation. In conclusion, autophagy, a gatekeeper of cell transformation, plays dual roles in Ras-overexpressed cells [45,46].

Altogether, we demonstrate a balance between BNIP3-mediated autophagy and H-*ras*^{val12}–induced tumorigenesis. We also reveal that BNIP3-mediated autophagy suppresses H-*ras*^{val12}–induced cell transformation and tumorigenesis *in vivo* through inhibition of cell proliferation. The threshold of autophagy as well as the temporal regulation of autophagy by H-*ras*^{val12} is involved in H-*ras*^{val12}–induced tumorigenesis.

Acknowledgments

The authors thank Drs N. Mizushima and T. Yahsimori for providing the plasmids pHA-Atg5 and ptfLC3. For the senescence experiment, the authors thank Dr. Y. L. Chen for providing the positive control and the senescence marker and P. Wilder for critical reading of the article.

References

[1] Maiuri MC, Zalckvar E, Kimchi A, and Kroemer G (2007). Self-eating and self-killing: crosstalk between autophagy and apoptosis. *Nat Rev Mol Cell Biol* **8**, 741–752.

[2] Mizushima N (2007). Autophagy: process and function. *Genes Dev* **21**, 2861–2873.

[3] Yoshimori T (2004). Autophagy: a regulated bulk degradation process inside cells. *Biochem Biophys Res Commun* **313**, 453–458.

[4] Lamark T, Kirkin V, Dikic I, and Johansen T (2009). NBR1 and p62 as cargo receptors for selective autophagy of ubiquitinated targets. *Cell Cycle* **8**, 1986–1990.

[5] Mathew R, Karp CM, Beaudoin B, Vuong N, Chen G, Chen HY, Bray K, Reddy A, Bhanot G, Gelinas C, et al. (2009). Autophagy suppresses tumorigenesis through elimination of p62. *Cell* **137**, 1062–1075.

[6] Liang C, Lee JS, Inn KS, Gack MU, Li Q, Roberts EA, Vergne I, Deretic V, Feng P, Akazawa C, et al. (2008). Beclin1-binding UVRAG targets the class C Vps complex to coordinate autophagosome maturation and endocytic trafficking. *Nat Cell Biol* **10**, 776–787.

[7] Levine B (2007). Cell biology: autophagy and cancer. *Nature* **446**, 745–747.

[8] Ogier-Denis E and Codogno P (2003). Autophagy: a barrier or an adaptive response to cancer. *Biochim Biophys Acta* **1603**, 113–128.

[9] Liu HS, Scrable H, Villaret DB, Lieberman MA, and Stambrook PJ (1992). Control of Ha-*ras*–mediated mammalian cell transformation by *Escherichia coli* regulatory elements. *Cancer Res* **52**, 983–989.

[10] Liu HS, Chen CY, Lee CH, and Chou YI (1998). Selective activation of oncogenic Ha-ras–induced apoptosis in NIH/3T3 cells. *Br J Cancer* **77**, 1777–1786.

[11] Yong HY, Hwang JS, Son H, Park HI, Oh ES, Kim HH, Kim do K, Choi WS, Lee BJ, Kim HR, et al. (2011). Identification of H-Ras–specific motif for the activation of invasive signaling program in human breast epithelial cells. *Neoplasia* **13**, 98–107.

[12] Wakasaki T, Masuda M, Niiro H, Jabbarzadeh-Tabrizi S, Noda K, Taniyama T, Komune S, and Akashi K (2010). A critical role of c-Cbl–interacting protein of 85 kDa in the development and progression of head and neck squamous cell carcinomas through the *ras*-ERK pathway. *Neoplasia* **12**, 789–796.

[13] Jiang R, Cabras G, Sheng W, Zeng Y, and Ooka T (2009). Synergism of BARF1 with Ras induces malignant transformation in primary primate epithelial cells and human nasopharyngeal epithelial cells. *Neoplasia* **11**, 964–973.

[14] Shima Y, Okamoto T, Aoyama T, Yasura K, Ishibe T, Nishijo K, Shibata KR, Kohno Y, Fukiage K, Otsuka S, et al. (2007). *In vitro* transformation of mesenchymal stem cells by oncogenic H-*ras*^{val12}. *Biochem Biophys Res Commun* **353**, 60–66.

[15] Ogier-Denis E, Pattingre S, El Benna J, and Codogno P (2000). Erk1/2–dependent phosphorylation of Gα-interacting protein stimulates its GTPase accelerating activity and autophagy in human colon cancer cells. *J Biol Chem* **275**, 39090–39095.

[16] Elgendy M, Sheridan C, Brumatti G, and Martin SJ (2011). Oncogenic *ras*-induced expression of Noxa and Beclin-1 promotes autophagic cell death and limits clonogenic survival. *Mol Cell* **42**, 23–35.

[17] Furuta S, Hidaka E, Ogata A, Yokota S, and Kamata T (2004). Ras is involved in the negative control of autophagy through the class I PI3-kinase. *Oncogene* **23**, 3898–3904.

[18] Byun JY, Yoon CH, An S, Park IC, Kang CM, Kim MJ, and Lee SJ (2009). The Rac1/MKK7/JNK pathway signals upregulation of Atg5 and subsequent autophagic cell death in response to oncogenic Ras. *Carcinogenesis* **30**, 1880–1888.

[19] Martin SJ (2011). Oncogene-induced autophagy and the Goldilocks principle. *Autophagy* **7**, 1–2.

[20] Azad MB and Gibson SB (2010). Role of BNIP3 in proliferation and hypoxia-induced autophagy: implications for personalized cancer therapies. *Ann NY Acad Sci* **1210**, 8–16.

[21] Rikka S, Quinsay MN, Thomas RL, Kubli DA, Zhang X, Murphy AN, and Gustafsson AB (2011). Bnip3 impairs mitochondrial bioenergetics and stimulates mitochondrial turnover. *Cell Death Differ* **18**, 721–731.

[22] Thomas RL, Kubli DA, and Gustafsson AB (2011). Bnip3-mediated defects in oxidative phosphorylation promote mitophagy. *Autophagy* **7**, 721–731.

[23] Vande Velde C, Cizeau J, Dubik D, Alimonti J, Brown T, Israels S, Hakem R, and Greenberg AH (2000). BNIP3 and genetic control of necrosis-like cell death through the mitochondrial permeability transition pore. *Mol Cell Biol* **20**, 5454–5468.

[24] Pedersen M, Lofstedt T, Sun J, Holmquist-Mengelbier L, Pahlman S, and Ronnstrand L (2008). Stem cell factor induces HIF-1α at normoxia in hematopoietic cells. *Biochem Biophys Res Commun* **377**, 98–103.

[25] Galang CK, Der CJ, and Hauser CA (1994). Oncogenic Ras can induce transcriptional activation through a variety of promoter elements, including tandem c-Ets-2 binding sites. *Oncogene* **9**, 2913–2921.

[26] Yeh HH, Wu CH, Giri R, Kato K, Kohno K, Izumi H, Chou CY, Su WC, and Liu HS (2008). Oncogenic Ras-induced morphologic change is through MEK/ERK signaling pathway to downregulate Stat3 at a posttranslational level in NIH3T3 cells. *Neoplasia* **10**, 52–60.

[27] Yeh HH, Giri R, Chang TY, Chou CY, Su WC, and Liu HS (2009). Ha-*ras* oncogene-induced Stat3 phosphorylation enhances oncogenicity of the cell. *DNA Cell Biol* **28**, 131–139.

[28] Tseng YS, Tzeng CC, Huang CY, Chen PH, Chiu AW, Hsu PY, Huang GC, Wang YC, and Liu HS (2006). Aurora-A overexpression associates with Ha-*ras* codon-12 mutation and blackfoot disease endemic area in bladder cancer. *Cancer Lett* **241**, 93–101.

[29] Kimura S, Noda T, and Yoshimori T (2007). Dissection of the autophagosome maturation process by a novel reporter protein, tandem fluorescent-tagged LC3. *Autophagy* **3**, 452–460.

[30] Zuber J, Tchernitsa OI, Hinzmann B, Schmitz AC, Grips M, Hellriegel M, Sers C, Rosenthal A, and Schafer R (2000). A genome-wide survey of RAS transformation targets. *Nat Genet* **24**, 144–152.

[31] Bellot G, Garcia-Medina R, Gounon P, Chiche J, Roux D, Pouyssegur J, and Mazure NM (2009). Hypoxia-induced autophagy is mediated through hypoxia-inducible factor induction of BNIP3 and BNIP3L via their BH3 domains. *Mol Cell Biol* **29**, 2570–2581.

[32] Zhang H, Bosch-Marce M, Shimoda LA, Tan YS, Baek JH, Wesley JB, Gonzalez FJ, and Semenza GL (2008). Mitochondrial autophagy is an HIF-1–dependent adaptive metabolic response to hypoxia. *J Biol Chem* **283**, 10892–10903.

[33] Prabhakaran K, Li L, Zhang L, Borowitz JL, and Isom GE (2007). Upregulation of BNIP3 and translocation to mitochondria mediates cyanide-induced apoptosis in cortical cells. *Neuroscience* **150**, 159–167.

[34] Quinsay MN, Lee Y, Rikka S, Sayen MR, Molkentin JD, Gottlieb RA, and Gustafsson AB (2010). Bnip3 mediates permeabilization of mitochondria and release of cytochrome *c* via a novel mechanism. *J Mol Cell Cardiol* **48**, 1146–1156.

[35] Mazure NM and Pouyssegur J (2009). Atypical BH3-domains of BNIP3 and BNIP3L lead to autophagy in hypoxia. *Autophagy* **5**, 868–869.

[36] Scott RC, Juhasz G, and Neufeld TP (2007). Direct induction of autophagy by Atg1 inhibits cell growth and induces apoptotic cell death. *Curr Biol* **17**, 1–11.

[37] Wang RC and Levine B (2010). Autophagy in cellular growth control. *FEBS Lett* **584**, 1417–1426.

[38] Mizushima N, Levine B, Cuervo AM, and Klionsky DJ (2008). Autophagy fights disease through cellular self-digestion. *Nature* **451**, 1069–1075.

[39] Denoyelle C, Abou-Rjaily G, Bezrookove V, Verhaegen M, Johnson TM, Fullen DR, Pointer JN, Gruber SB, Su LD, Nikiforov MA, et al. (2006). Anti-oncogenic role of the endoplasmic reticulum differentially activated by mutations in the MAPK pathway. *Nat Cell Biol* **8**, 1053–1063.

[40] Lee KE and Bar-Sagi D (2010). Oncogenic KRas suppresses inflammation-associated senescence of pancreatic ductal cells. *Cancer Cell* **18**, 448–458.

[41] Narita M and Young AR (2009). Autophagy facilitates oncogene-induced senescence. *Autophagy* **5**, 1046–1047.

[42] Ullman E, Fan Y, Stawowczyk M, Chen HM, Yue Z, and Zong WX (2008). Autophagy promotes necrosis in apoptosis-deficient cells in response to ER stress. *Cell Death Differ* **15**, 422–425.

[43] Shao J, Sheng H, DuBois RN, and Beauchamp RD (2000). Oncogenic Ras-mediated cell growth arrest and apoptosis are associated with increased ubiquitin-dependent cyclin D1 degradation. *J Biol Chem* **275**, 22916–22924.

[44] Yousefi S and Simon HU (2009). Autophagy in cancer and chemotherapy. *Results Probl Cell Differ* **49**, 183–190.

[45] Lock R, Roy S, Kenific CM, Su JS, Salas E, Ronen SM, and Debnath J (2011). Autophagy facilitates glycolysis during Ras-mediated oncogenic transformation. *Mol Biol Cell* **22**, 165–178.

[46] Guo JY, Chen HY, Mathew R, Fan J, Strohecker AM, Karsli-Uzunbas G, Kamphorst JJ, Chen G, Lemons JM, Karantza V, et al. (2011). Activated Ras requires autophagy to maintain oxidative metabolism and tumorigenesis. *Genes Dev* **25**, 460–470.

[47] Kim MJ, Woo SJ, Yoon CH, Lee JS, An S, Choi YH, Hwang SG, Yoon G, and Lee SJ (2011). Involvement of autophagy in oncogenic K-*Ras*–induced malignant cell transformation. *J Biol Chem* **286**, 12924–12932.

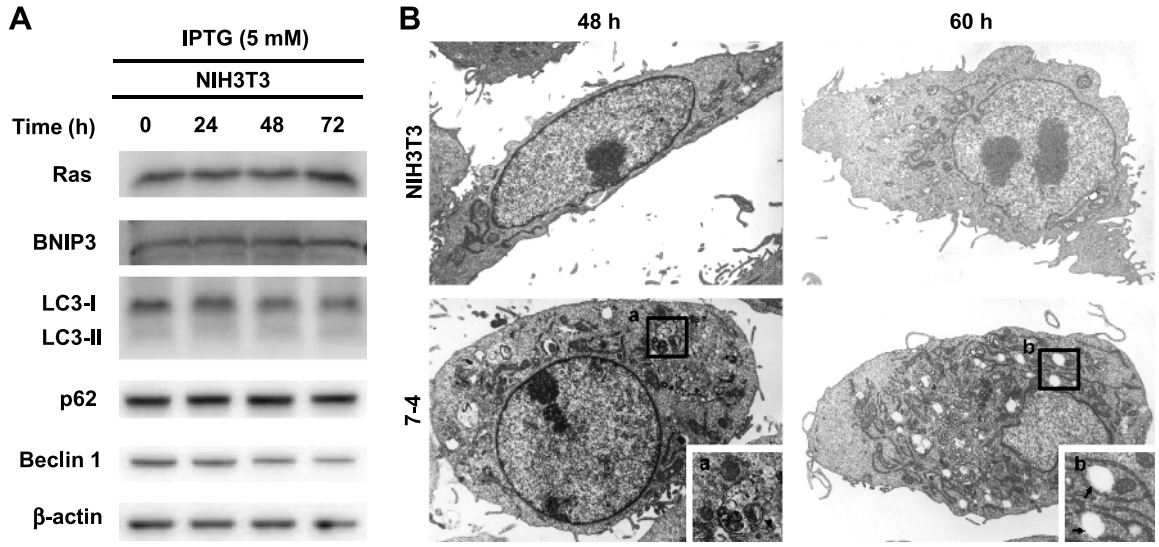

Figure W1. H-*ras*^{val12} induces autophagosome formation. (A) The NIH3T3 cells were treated with IPTG for various times and protein was extracted, and the expression levels of Ras, BNIP3, LC3, p62, and Beclin-1 were evaluated by immunoblot analysis using specific antibodies. β-Actin was used as an internal control. (B) NIH3T3 and 7-4 cells after IPTG treatment for 48 and 60 hours were sectioned and investigated under transmission electron microscopy. The higher magnification is shown in a and b. The arrowhead points the autophagosome, and the arrow points the autophagolysosome-like vesicles.

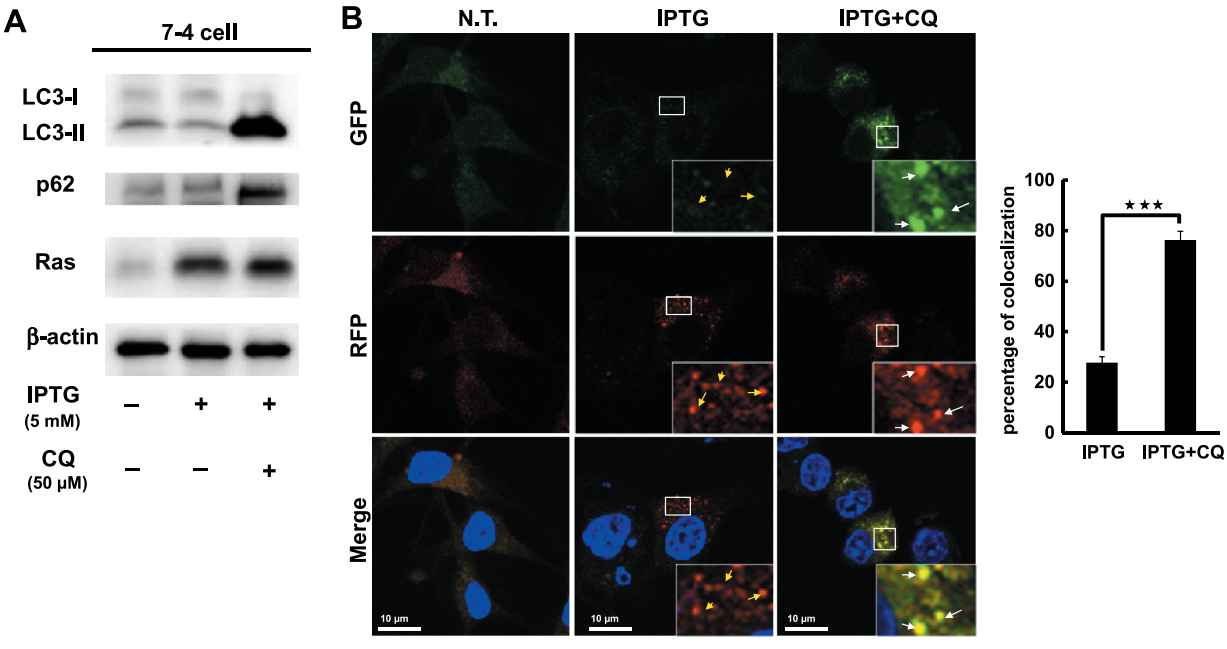

Figure W2. H-*ras*^{val12} induces the autophagic flux. (A) The 7-4 cells were treated with lysosome inhibitor CQ (50 μM) at 48 hours after IPTG induction for 24 hours. The protein extracted was assessed for the expression levels of LC3 and p62 by immunoblot analysis. (B) The 7-4 cells were transfected with ptfLC3 plasmid. After transfection for 24 hours, cells were treated with IPTG for another 48 hours. The 7-4 cells were treated with CQ (50 μM) at 48 hours after IPTG induction for 24 hours and investigated under a confocal microscope. White arrow points the spot showing autophagosomes (red [RFP] and green [GFP]), yellow arrow points the spot showing autophagolysosomes (red [RFP] only). Colocalization of mRFP and GFP puncta was quantified and shown as the percentage of the total number of mRFP puncta. Twenty cells were counted in each view, and three views were investigated.

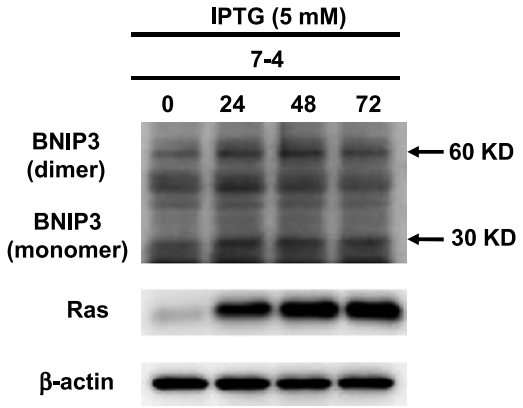

Figure W3. The expression levels of monomer and dimmer of BNIP3 are increased under H-*ras*^{val12} overexpression conditions. The 7-4 cells were treated with IPTG from 24 to 72 hours, and protein was extracted and the expression levels of BNIP3, Ras, and β-actin were evaluated by immunoblot analysis with specific antibodies. The anti-BNIP3 antibody (ab10433) was from Abcam.

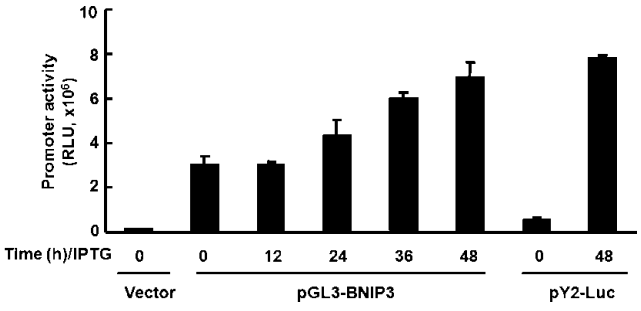

Figure W4. H-*ras*^{val12} induces BNIP3 promoter activity. The 7-4 cells were transfected with plasmid pGL3-BNIP3 or pY2Luc (0.2 μg/each), and the promoter activity at various times after IPTG treatment was measured by luciferase activity assay. The pY2Luc is the reporter plasmid for measuring Ras activity and was used as a positive control. The plasmid pGL3 was used as the vector control.

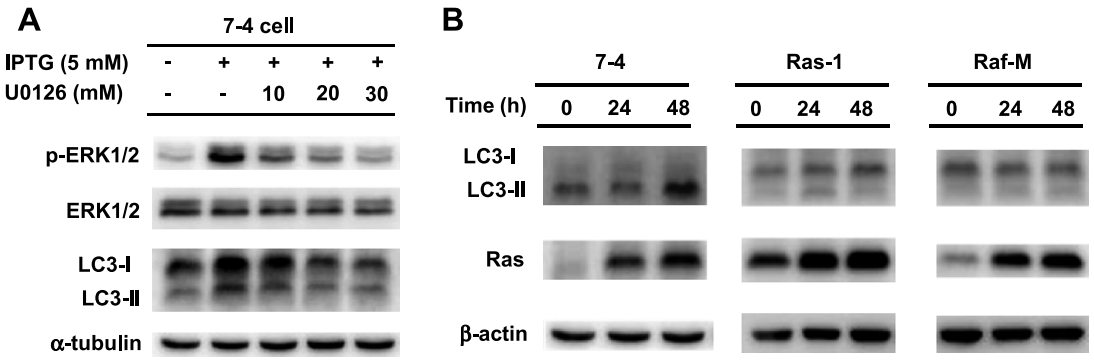

Figure W5. Ras induces autophagy through ERK pathway. (A) The 7-4 cells were treated with various dosages of U0126 in the presence of IPTG. The expression levels of phosphorylated ERK (p-ERK) and LC3 protein were evaluated at 48 hours after treatment. α-Tubulin was used as the internal control. (B) The 7-4 cell and its derivates Ras-1 (containing DN-*ras*) and Raf-M (containing DN–*raf*-1) were treated with IPTG for 24, 48, and 72 hours. The protein was extracted for evaluation of LC3 and Ras expression by Western blot analysis. β-Actin was used as an internal control.

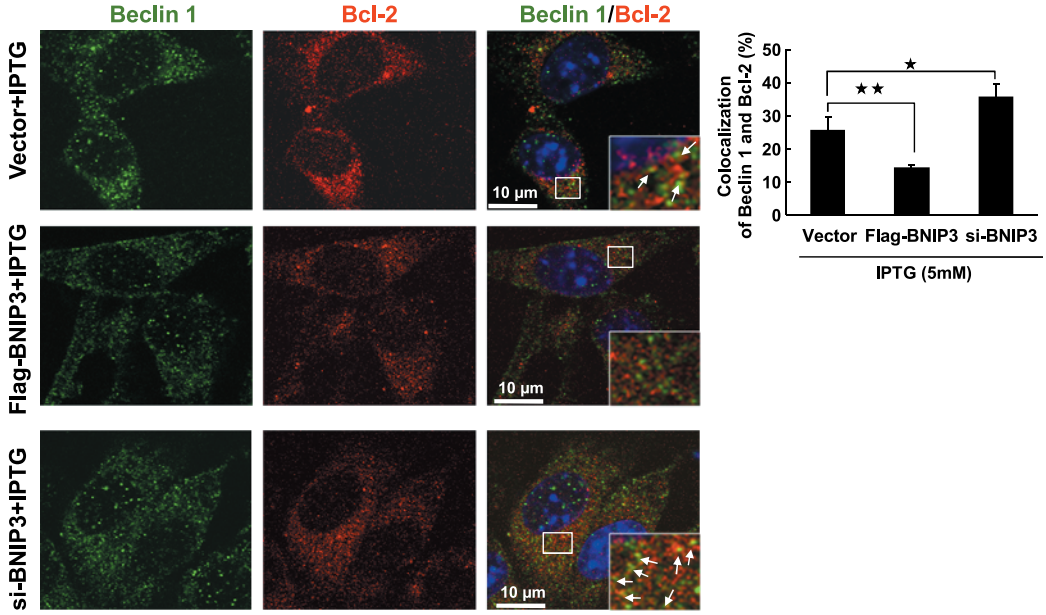

Figure W6. BNIP3 competes with Beclin 1 to bind with Bcl-2. The 7-4 cells in the presence of IPTG were transfected with siRNA of BNIP3, pFLAG-BNIP3, or pFlag-CMV2 (Vector) for 48 hours. Colocalization of Beclin 1 (green) and Bcl-2 (red) was assessed and quantified.

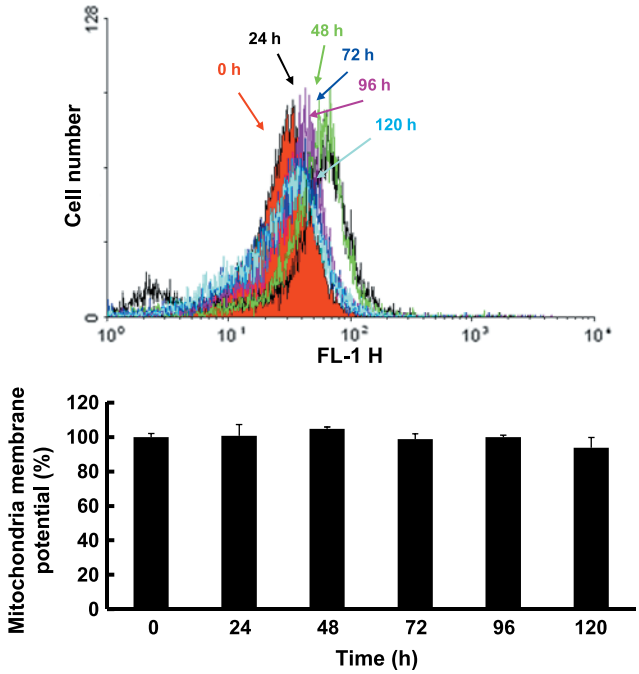

Figure W7. H-*ras*^{val12} overexpression does not decrease mitochondria membrane potential in NIH3T3 cells. After IPTG treatment of 7-4 cells for 0, 24, 48, 72, 96, and 120 hours, DiOC6 (318426; Sigma) dye that contains fluorescence (1 μM) was used to analyze mitochondria membrane potential by flow cytometry. The cell treated with IPTG for 0 hour was used as the control.

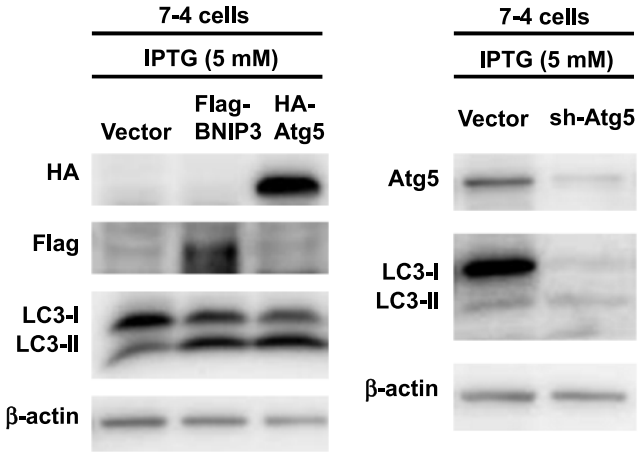

Figure W8. BNIP3 and Atg5 were expressed or silenced in the transected cells. The 7-4 cells were transfected with pFlag-BNIP3 plasmid DNA (4 μg), pHA-Atg5, psh-Atg5 (4 μg), or pFlag-CMV2 (Vector) for 48 hours. The expression levels of Flag-BNIP3, HA-Atg5, LC3, and Atg5 were detected by Western blot analysis using antibodies against Flag (no. 2368; Cell Signaling), anti-HA (H6908; Sigma), LC3, and Atg5.

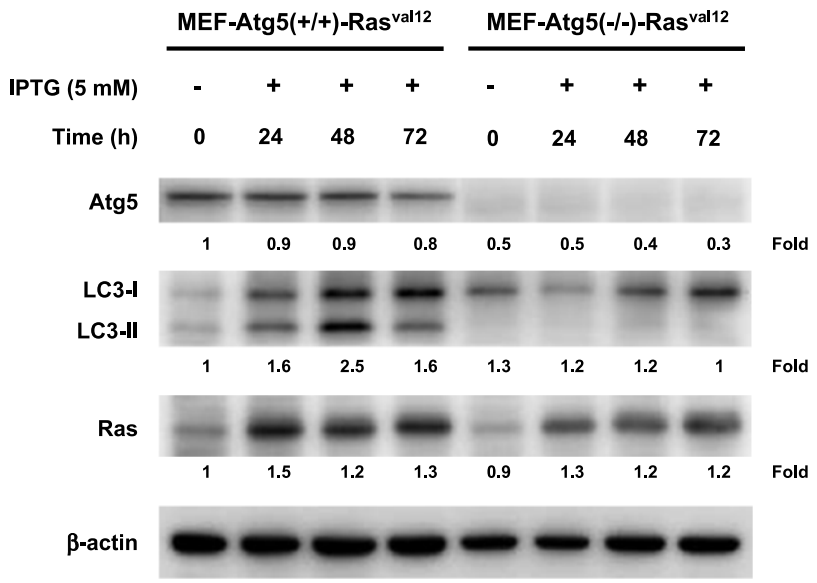

Figure W9. The inducible Ras system was established in MEF-Atg5(+/+) and MEF-Atg5(−/−) cell lines and ras induces autophagy in MEF-Atg5(+/+) cells. MEF-Atg5(+/+) and MEF-Atg5(−/−) cells were transfected with plasmid pSVlacO*ras* and placI, and H-*ras*–inducible cell lines after G418 selection were established. These cell lines were treated with IPTG (5 mM) for 0, 24, 48, and 72 hours, and the expression of Atg5, LC3, Ras, and β-actin was detected with specific antibodies and analyzed by immunoblot analysis. β-Actin was used as an internal control.

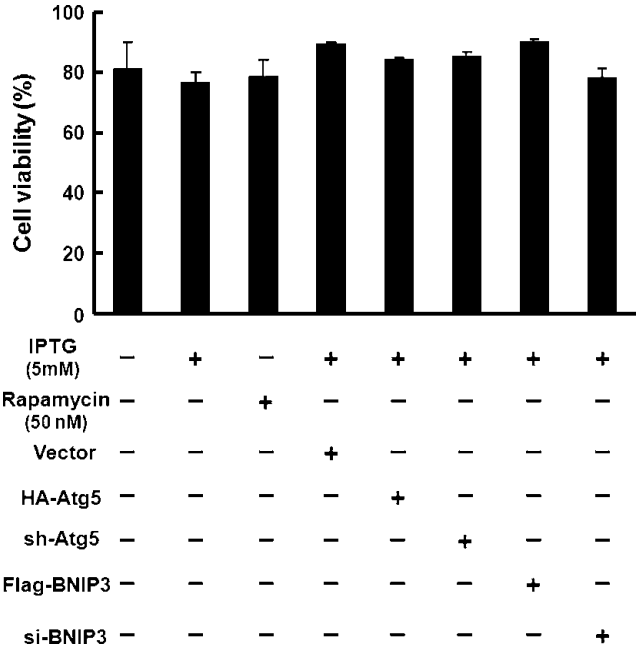

Figure W10. H-*ras*^{val12}–induced autophagy does not trigger cell death. The 7-4 cells in the presence or absence of IPTG were treated with rapamycin (50 nM), pFlag-BNIP3 (4 μg), psh-Atg5 (4 μg), or si-BNIP3 (200 mM) for 48 hours and then labeled with PI (0.04 mg/ml). Cell viability was evaluated by flow cytometry analysis at 72 hours after treatment.

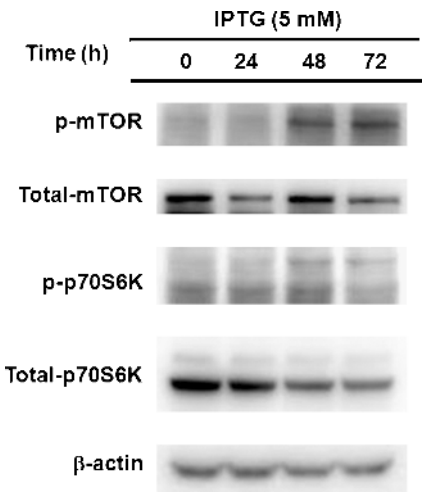

Figure W11. The mTOR signaling pathway is activated by H-*ras*^{val12}. After IPTG treatment of 7-4 cells for 0, 24, 48, and 72 hours, the expressions of mTOR signaling pathway–related proteins (mTOR, p-mTOR, and its downstream protein p70^{S6K} and p-p70^{S6K}) were evaluated using specific antibodies by Western blot analysis. The following antibodies were used: mTOR (no. 2983; Cell Signaling), p-mTOR (no. 2971; Cell Signaling), p70S6 kinase (no. 2708; Cell Signaling), and p-p70S6 kinase (no. 9206; Cell Signaling). β-Actin was used as an internal control.

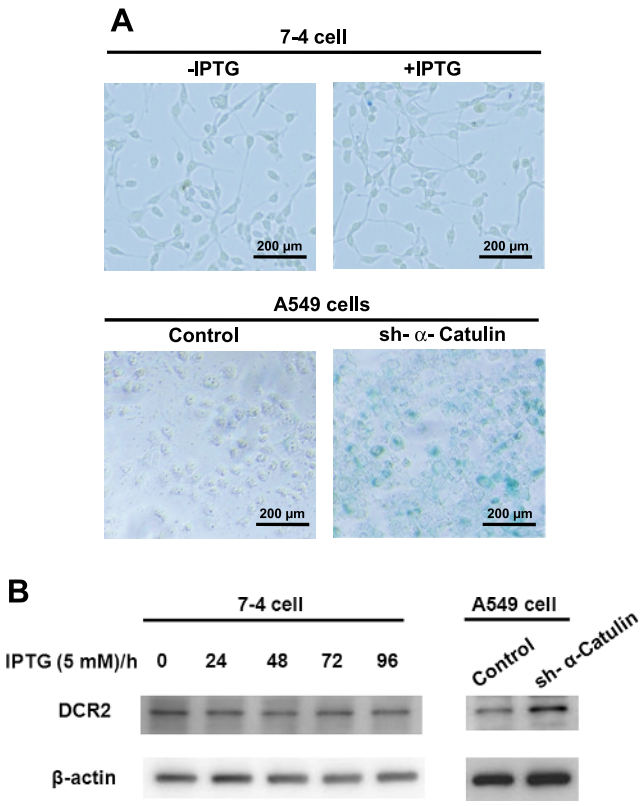

Figure W12. H-*ras*^{val12} overexpression does not induce senescence in NIH3T3 cells. (A) The 7-4 cells were treated with IPTG for 72 hours, and senescence was detected by expression of SA-β-galactosidase. α-Catulin expression in lung adenocarcinoma cell line (A549) is knocked down by lentiviral expression of α-Catulin shRNA, which is used as a senescence control cell line. (B) The 7-4 cells were treated with IPTG for various times, and protein was extracted. The expression levels of decoy receptor 2 (DCR2), a senescence marker, was detected by Western blot analysis.

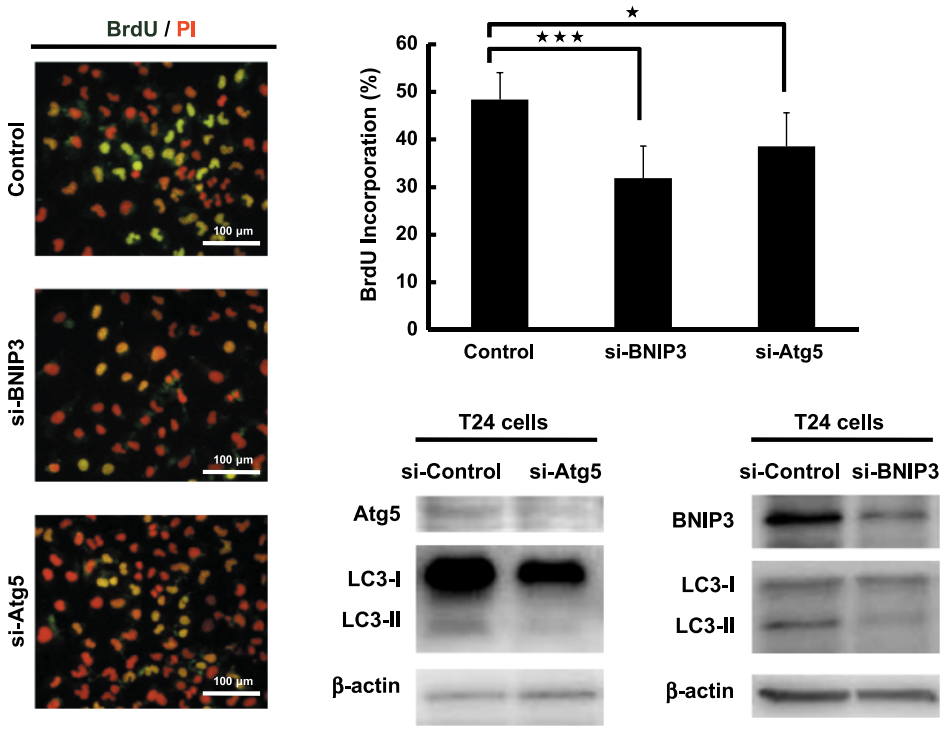

Figure W13. H-*ras*^{val12} overexpression–induced autophagy suppresses cell proliferation in human bladder cancer cell line. T24 cells in the presence of IPTG were transiently transfected with RNAi-negative control, si-Atg5, or si-BNIP3 (200 mM) for 48 hours. Cell proliferation was determined by BrdU (0.02 g/ml) incorporation for 30 minutes. Anti-BrdU antibody and PI were used to label the treated cells for cell proliferation and nuclei, respectively. The expression levels of Atg5, BNIP3, and LC3 were detected with specific antibodies by Western blot analysis.